

LIBRARIES
MICHIGAN STATE UNIVERSITY
EAST LANSING, MICH 48824-1048

This is to certify that the
thesis entitled

FABRICATION, CHARACTERIZATION, AND STAMP
THERMOFORMING OF NATURAL FIBER
POLYPROPYLENE COMPOSITES CONTAINING KENAF
FIBERS

presented by

STACEY ANNE YANKOVICH

has been accepted towards fulfillment
of the requirements for the

M.S. degree in Mechanical Engineering



Major Professor's Signature

11 / 30 / 04

Date

PLACE IN RETURN BOX to remove this checkout from your record.
TO AVOID FINES return on or before date due.
MAY BE RECALLED with earlier due date if requested.

DATE DUE	DATE DUE	DATE DUE

**FABRICATION, CHARACTERIZATION, AND STAMP THERMOFORMING
OF NATURAL FIBER POLYPROPYLENE COMPOSITES CONTAINING
KENAF FIBERS**

by

Stacey Anne Yankovich

A THESIS

Submitted to
Michigan State University
in partial fulfillment of the requirements
for the degree of

MASTER OF SCIENCE

Department of Mechanical Engineering

2004

ABSTRACT

FABRICATION, CHARACTERIZATION, MODELING, AND STAMP THERMOFORMING OF NATURAL FIBER POLYPROPYLENE COMPOSITES CONTAINING KENAF FIBERS

By

Stacey Anne Yankovich

Ecological concerns have led to the need for an increase in the use of environmentally friendly materials. Kenaf fiber-polypropylene composites have been shown to have an optimal fabrication process utilizing a layered “sifting” process of both matrix and fibers, followed by compression molding. Mechanical property tests have shown that these natural fiber composites possess superior mechanical properties to natural fiber composites formed in other recent studies, as well as significantly higher Modulus/Cost and Specific Modulus than E-Glass composites. Using the properties determined during testing as input parameters an attempt was made to numerically model the behavior during forming. The kenaf-polypropylene composites were also easily thermoformed into hemispherical cups, showing expected wrinkling behavior. Comparing numerical modeling to the experimental results has proven that a two preferred fiber orientation linear elasticity model is not able to accurately capture the behavior of the kenaf fibers. Future modeling work is necessary, but at this time it may be concluded that kenaf-polypropylene composites are a viable substitute for many glass fiber composite automotive and housing applications.

DEDICATION

This thesis is dedicated to my parents, Mr. Michael Yankovich and Mrs. Denise Yankovich, my brother Matthew Yankovich, and all of the friends who have helped along the way. Thank you.

ACKNOWLEDGMENTS

I express my sincere appreciation to Dr. Farhang Pourboghrat, Dr. Michael Zampaloni, and Mr. Nader Abedrabbo for all of their patience, guidance, and support throughout my research. I would also like to acknowledge Dr. Manju Misra and Dr. Masud Huda of the Michigan State University Composite Materials and Structures Center for sharing their knowledge and direction in dealing with natural fiber composites.

I would like to acknowledge Mr. Mike Rich and Mr. Kelby Thayer for their support and training with various equipment for experiments.

I would like to thank my colleague, Mrs. Barbara Rodgers, for all of her contributions and support throughout this project.

I would like to thank my family and friends for all of the love, encouragement, and patience. You have all been wonderful.

TABLE OF CONTENTS

LIST OF TABLES	vi
LIST OF FIGURES	vii
CHAPTER 1	
INTRODUCTION	1
CHAPTER 2	
LITERATURE REVIEW	6
2.1 Natural Fiber Composites	6
2.2 Coupling Agents	13
2.3 Forming Composites	18
2.4 Modeling	19
CHAPTER 3	
FABRICATION OF NATURAL FIBER COMPOSITES	23
3.1 Fabrication of Woodfiber Composites	23
3.2 Fabrication of Kenaf-Polypropylene Composites	25
CHAPTER 4	
CHARACTERIZATION OF MATERIAL PROPERTIES	35
4.1 Squeeze Flow Testing	35
4.2 Tensile and Flexural Testing	39
CHAPTER 5	
EXPERIMENTAL WORK	47
5.1 Apparatus Design and Setup	47
5.2 Thermoforming Results	49
CHAPTER 6	
NUMERICAL ANALYSIS	53
6.1 Numerical Analysis Theory	53
6.2 Properties for the Numerical Model	
6.3 Mass/Density Scaling Sensitivity Analysis	57
6.4 Initial Fiber Volume Fraction Sensitivity Analysis	60
6.5 Shear Modulus Sensitivity Analysis	61
6.6 Transverse Shear Stiffness Sensitivity Analysis	62
6.7 Numerical Analysis Final Results	64

CHAPTER 7	
NEW DIE DESIGN.....	66
7.1 Design Features	66
7.2 Punch Options	70
7.3 Numerical Model.....	71
7.4 Numerical Analysis Results	74
CHAPTER 8	
FUTURE WORK.....	76
8.1 Future Experimentation	83
8.2 Future Numerical Work.....	84
CHAPTER 9	
CONCLUSIONS	85
REFERENCES	86

LIST OF TABLES

	Page
Table 3.1 Optimal Quantities of Composite Components	33
Table 4.1 Conditions for Tensile and Flexural Tests	41
Table 4.2 Mechanical Properties from Tensile and Flexural Tests	44
Table 5.1 Thermoforming Parameters	51
Table 6.1 Input Parameters for VUMAT	46
Table 6.2 Additional Input Parameters	46
Table 6.3 Density Scaling Sensitivity Analysis Results	58
Table 6.4 Initial Fiber Volume Fraction Sensitivity Analysis Results	60
Table 6.5 Shear Modulus Sensitivity Analysis Results	62
Table 6.6 Transverse Shear Stiffness Sensitivity Analysis Results	64
Table 6.7 Summary of all Numerical Simulation Results	65

LIST OF FIGURES

	Page
Figure 3.1 Woodfiber reinforced polypropylene composites	24
Figure 3.2 Carver Laboratory Press used for compression molding	27
Figure 3.3 Composite fabricated by sandwiching layers with long fibers.....	27
Figure 3.4 Composite fabricated by sandwiching layers with chopped fibers.....	28
Figure 3.5 Kenaf-polypropylene composites fabricated by dry mixing.....	28
Figure 3.6 Kenaf-polypropylene composite fabricated by multiple layering of powder and fibers.....	30
Figure 3.7 Twelve inch kenaf-polypropylene composite fabricated by multiple layering of powder and fibers	30
Figure 3.8 Tetrahedron Smart Press used for compression molding	31
Figure 3.9 Final kenaf-polypropylene biocomposite with 30% fiber by weight.....	32
Figure 3.10 Flow chart of optimal fabrication process.....	34
Figure 4.1 Schematic of Squeeze Flow Test experimental setup.....	36
Figure 4.2 Squeeze flow test sample before (right) and after (left) compression.....	37
Figure 4.3 Plot of average normalized squeeze flow data for all 24 samples.....	38
Figure 4.4 Plot of averaged normalized squeeze flow data using best samples.....	38

Figure 4.5	UTS Machine.....	41
Figure 4.6	Stress-strain curve for PP with 3% MAPP	42
Figure 4.7	Stress-strain curve for 30% Kenaf, 67% PP and 3% MAPP at 40°	42
Figure 4.8	Stress-strain curve for 30% Kenaf, 67% PP and 3% MAPP at 170°	43
Figure 4.9	Strain-load curve for 30% kenaf, 67% PP and 3% MAPP at 40°	43
Figure 4.10	Strain-load curve for 30% kenaf, 67% PP and 3% MAPP at 170°	44
Figure 4.11	Comparison of the tensile strength of kenaf-PP composites to other natural fiber composites	
Figure 4.12	Comparison of the flexural strength of kenaf-PP composites to other natural fiber composites	
Figure 4.13	Comparison of Specific Modulus for various fibers.....	
Figure 4.14	Comparison of Modulus per Cost of various fibers	
Figure 5.1	Double-action servo press 75 manufactured by Interlaken Technology Corporation	48
Figure 5.2	Schematic of stamp thermoforming setup	48
Figure 5.3	Modified Interlaken press for stamp thermoforming.....	49
Figure 5.4	Kenaf-MAPP composite formed in ambient conditions.....	50
Figure 5.5	Typical thermoformed kenaf-MAPP composite.....	52
Figure 6.1	Undeformed model of the thermoforming process using ABAQUS	54
Figure 6.2	Undeformed mesh of the blank in ABAQUS	55
Figure 6.3	Numerical simulation results with density of	

993E2 kg/m ³	58
Figure 6.4 Internal (left) and Kinetic (right) Energy plots of numerical simulation with density of 993E2 kg/m ³	59
Figure 6.5 Comparison of numerical results with initial fiber volume fractions of 0.4 (left), 0.5 (center), and 0.6 (right).....	61
Figure 6.6 Comparison of numerical results with Shear Modulus of 1.43E6 Pa (left), 1.43E7 Pa (center), and 1.43E9 Pa (right)	62
Figure 6.7 Comparison of numerical results with Transverse Shear Stiffness of 1.23E6 Pa (left), 1.0E3 Pa (center), and 1.23E9 Pa (right).....	63
Figure 7.1 New die design, exploded view	67
Figure 7.2 New die design of top plate	68
Figure 7.3 New die design of bottom plate	68
Figure 7.4 New die design of top die	69
Figure 7.5 New die design of bottom die	69
Figure 7.6 New die design of insert.....	70
Figure 7.7 Original oilpan design (right) and modified oilpan for formability tests	71
Figure 7.8 ABAQUS model of oilpan punch with match shaped dies.....	73
Figure 7.9 Numerical simulation results for oilpan punch with circular inserts	74
Figure 7.10 Numerical simulation results for oilpan punch with matched inserts.....	74

Chapter 1

INTRODUCTION

Ecological concerns have recently led to a high demand for more environmentally friendly materials. Instead of the traditional dependence on fossil fuel based processes, industry has been moving towards natural materials. Previously, composites made of glass and carbon fibers replaced many metal applications by supplying the benefits of low cost and high strength properties. The processes associated with these materials have been critically evaluated recently [1]. An enormous amount of attention has been given to the fabrication and properties of biocomposites. The Technology Road Map for Plant/Crop-based Renewable Resources 2020, which is sponsored by the U.S. Department of Energy, has set a goal to increase plant-derived renewable sources to 10% of all basic chemical building blocks by 2020, and up to 50% by 2050 [2].

A biocomposite can be defined as a combination of biofibers and bioplastics, both being derived from renewable resources. The main concern when dealing with these materials has been degradation due to environment. An assurance that the composite will maintain the desired properties throughout its lifetime, yet be biodegradable when use is finished is necessary [3]. Different types of surface treatments are being developed, as well as possible sandwich structures with a biocomposite core between metal sheets. The automotive and aerospace industries are both extremely interested in using more natural fiber reinforced biocomposites. In order to reduce vehicle weight, automotive

companies have shifted from steel to aluminum to plastics and now composites. This has led to predictions that in the near future plastics and polymer composites will comprise approximately 15% of car total weight [4].

True bioplastics are constantly being researched and improved. Different types of biosynthetic polymers include aliphatic polyesters, polyester amides, starch plastics, and soy plastics. Due to the fact that these materials are so new and still being developed, they are currently only viable in terms of price and performance for components of packaging [5]. In the very near future, these biopolymers will become crucial in the development of biocomposites. During this study, polypropylene will be used instead of a biopolymer. The biopolymers are not used because there are still many factors to be resolved with the natural fibers, and the biopolymers are still in development. Once viable composites are easily fabricated and formed with a polypropylene matrix, the process of substituting a biopolymer will be more easily achieved.

Natural fibers that have been studied as replacements for glass and other non-biodegradable composites include flax, hemp, kenaf, and sisal [6]. These fibers are abundant, cheap, renewable, and biodegradable. Other advantages include low density, high toughness, comparable specific strength properties, reduction in tool wear, ease of separation, decrease in energy of fabrication, and CO₂ neutrality [7]. Additionally, insulation and sound absorption properties make these composites useful for housing and automotive applications [8,9].

Natural fibers can be split into two categories, bast and leaf. The bast fibers include kenaf, hemp, and flax; sisal is considered a leaf fiber. The bast

composites exhibit a superior flexural strength and Modulus of Elasticity (MOE), but the leaf composites show superior impact properties. Compared to glass fiber composites, the bast composites showed approximately the same flexural strength and a higher MOE [4].

The main drawback in using these natural fiber composites is the hydrophilic nature of the biofibres, causing problems of adhesion with the hydrophobic polymer matrix. The problem of adhesion is still a topic of research, but strong promise has been seen with the use of coupling agents and other chemical modifications [10]. Another problem is that high temperatures must be avoided due to the possibility of fiber degradation [11]. It is also important to note that natural fibers can vary immensely depending on many different factors. They are grown in nature and may easily vary in properties from plant to plant. The kenaf crop growing conditions have a direct and significant effect on the fiber dimensions and properties [12]. A single best method for fabrication of these composites has still not yet been proven, but this work will develop a method of fabrication, as well as showing the ability to form the composite into a useful part.

In order to form these composites into complex shapes at elevated temperatures there is a need for a specialized manufacturing process. Previous work has been done to find a method for forming continuous fiber and woven-fiber composites. The main problem with conventional stamping techniques has been wrinkling and distortion of the fibers. The process that has been proven to be able to lessen and even eliminate these problems is stamp thermo-hydroforming [13-15].

During the stamp thermo-hydroforming process, pressurized fluid is used to aid in the forming of the part. This process uses a punch, but fluid pressure forces the blank to conform to the punch shape and does not allow the material to wrinkle. The pressure applied is able to be controlled and varied throughout the process, giving optimum performance. The fluid in the chamber is also heated to forming temperature to additionally aid with the shaping of the material. No female die is necessary in this process, and, typically, no holding force is needed because of the pressurized fluid. Other advantages associated with this process include increased drawability of the blank, decreased tool wear because less energy is needed, decreased thinning of the part as compared to previous drawing processes, economic savings, improved surface finish, and the ability to conform to complex shapes [13-15].

In order to begin to optimize the stamp hydro-thermoforming process, the behavior of a material during a simple stamping process must be accurately modeled. This work will focus on accurately modeling the stamp thermoforming process and the wrinkling behavior of the material. The model developed will aid in finding the optimal fluid pressure amplitude curve to eliminate wrinkling without tearing. With an accurate model different holding forces and pressures may be experimented with much more easily, quickly, and inexpensively.

In the following, there will be a presentation of the current work and research regarding the areas of natural fiber composite properties and forming methods. This will be followed by a series of methods for fabrication of natural fiber and polypropylene composites, as well as the applications of these

composites in the hydroforming process. The mechanical properties of the natural fiber composite material will be determined by a series of tests, followed by the initial results obtained from experiments conducted using in-house stamp thermo-hydroforming equipment. The results of these experiments will finally be compared to a finite element simulation of the process and material behavior using a modified version of a previous code for glass-fiber reinforced composites. Numerical analysis for future work will also be completed using new dies that have been designed. The new dies feature an oil pan shaped punch, showing the ability of the material to conform to different complex geometries.

Chapter 2

LITERATURE REVIEW

In an effort to choose an appropriate natural fiber for the composites, a survey has been done of the past work including bast, leaf and woodfiber composites. Much work has been done to determine optimal fabrication methods, as well as to characterize biocomposites. The survey will begin with studies on different types of composites. Next, it will continue with composite performance enhancers. This will be followed by a short summary of forming that has been done. There are few known publications on the forming of these types of composites, which helps to show that this study is an original and necessary work. Finally, a review of previous modeling techniques for this type of composite materials will be given.

2.1 Natural Fiber Composites

Mckenzi and Yuritta (1979) [16] compared different types of woodfiber reinforced polymers. The purpose of their work was to determine if woodfiber has advantages as a reinforcing material over other fibrous materials. Comparisons were made with nylon, rayon, glass, and Kevlar to name a few. The short length of woodfiber leads to the conclusion that the bonding of the matrix with the fiber will be crucial. This is due to the fact that the full strength of the fiber will only be utilized if a strong bond is formed. Tensile tests were performed with woodfiber-polypropylene and woodfiber-polyethylene samples

with different percentages of fiber by mass. The results of these tests showed that with either of these polymers as the matrix and adequate impregnation, the fiber strength is able to be completely utilized.

A comparison of the benefits of woodfiber and glass fiber was also performed in this study. It was found that if the fiber volume fraction was the same for a glass fiber and a woodfiber composite, then the woodfiber composite would have to be 67% thicker than a glass fiber composite in order to have the same strength. This increased polymer matrix requirement reduces the cost benefit of woodfiber over glass, but there is also a possibility for reduction in matrix usage for low fiber content systems. Additionally, woodfiber provides advantages by consuming less energy during fiber manufacture and the potential for lower mass structures. The disadvantages of using woodfiber composites are poor water resistance, lower packaging efficiency, greater matrix usage in high fiber content systems, and unavailability in highly oriented forms.

Michell (1986) [17] did another study on different types of composites containing wood pulp fibers. The elastic properties of the composites were developed from the elastic properties of the components using the Rule of Mixtures. Michell has shown that wood pulp fibers are cheaper than other organic polymers and also lead to improvements of both the strength and tensile modulus of composites. He has shown that although the wood pulp fibers were already being used in thermoset applications, there also exists much opportunity for use as reinforcements in thermoplastic composites. Concerns of forest

destruction have led to a shift to more work on natural fibers, even though wood fibers have been shown to perform well.

Mohanty et al. (2000) [18] compiled an overview on the different biofibers, biopolymers, and biocomposites available up to that date. This study defined biocomposites and compared advantages and disadvantages of these materials (which were also defined in the Introduction section). Properties of many biodegradable polymers were also investigated and compared. Although the use of biodegradable polymers is outside the scope of the work in this thesis, this lays the groundwork for future work using these more environmentally friendly polymers. These will be necessary later due to the growing problem of waste and the need for environmentally friendly use of resources with the CO₂ neutrality aspect. The challenge ahead will be to find applications that use enough of the biocomposite material to make the prices competitive.

Different fiber-polymer composites were fabricated and tested in this work. The specific properties of natural fibers such as hemp, kenaf, jute, flax, and sisal were compared with traditional composite reinforcements. The prices of these natural fibers are very low as compared to synthetic fibers. The prices may vary depending on the yearly crop, but kenaf fiber is grown commercially in the United States, leading to some regularity. Additionally, the density of these fibers is shown to be much less, leading to strength/weight ratios comparable with those of such widely used materials as E-glass and Aramid.

From the testing of biocomposites in this study, the optimal fiber content proved to be approximately 30%. These natural fiber composite materials are

well suited for lightweight vehicle interior parts as well as other applications in railways, aircrafts, irrigation systems, furniture industries, and some sports and leisure items.

Wambua et al. (2003) [19] followed up by testing more natural fibers to see if they have the ability to replace glass. This study involved the properties of several different natural fiber-polypropylene composites. They used polypropylene with a very high melt flow index to help with fiber matrix adhesion difficulties and ensure proper wetting of the fibers. The composites were formed in 30cm squares using 3 layers of fibers with polypropylene sheets in between. The fibers were spread as randomly as possible. Each composite was wrapped in aluminum foil and preheated at 140°C for 20 minutes to reduce moisture content. Then the composites were pressed at 180°C and 5 bars for 2 minutes, and then cooled at the same pressure for 3 minutes. Samples were made with 40% fiber content of kenaf, coir, sisal, hemp, and jute.

After all the samples were fabricated, tensile and impact tests were run to compare the properties of these composites to those made with glass fiber. The tensile strengths all compared well with glass, except for the coir, but the only sample with the same flexural strength was hemp. It was shown with kenaf fibers that increasing fiber weight fraction increased ultimate strength, tensile modulus, and impact strength. However, the composites tested showed low impact strengths compared to glass mat composites. This study showed that natural fiber composites have a potential to replace glass in many applications that do not require very high load bearing capabilities.

Mishra et al. (2003) [20] continued studying the mechanical performance of biofiber/glass reinforcements, this time using a polyester matrix to create hybrids. This study used pineapple leaf (PALF) and sisal fibers with the addition of a small amount of glass. PALF and sisal fibers were chosen for their moderately high specific strengths and stiffness. The main problem in these composites, as with all natural fiber composites, is the lack of good fiber matrix adhesion and poor resistance to moisture. The addition of a small amount of glass was used to help with adhesion, and has been shown to have a positive hybrid effect, i.e. increasing properties. The conclusions of this study prove to be promising for future applications, but the addition of glass into the composites prevents them from being a fully environmentally friendly product. The goal of this research is to begin to make and prove the formability of natural fiber composites. Therefore, this data will not be used, yet still may be a direction to go in the future if the properties do not prove sufficient.

Mohanty et al. (2004) [21] delved further into natural fiber composites by investigating the effects of process engineering on the performance of the natural fiber composites. This study used biocomposites formed using chopped hemp fiber and cellulose ester biodegradable plastic. The effect of two different processing approaches was studied. Prior to both processes, the hemp fibers were dried to remove any additional moisture. During the first process, the chopped fiber (30% by weight) was mechanically mixed in a kitchen mixer for 30 minutes. The mechanical mixing was followed by compression molding using a picture-frame mold. The second process involved two steps, the first extrusion

process yielded pellets of cellulose acetate plastic (CAP). These pellets were then fed into a twin-screw extruder while chopped hemp fibers were also fed into the last zone of the extruder. This two-step process yielded thin strands of the composite, which were pelletized for injection molding. They were later injection molded into tensile test shaped coupons.

One of the main advantages of melt mixing is the superior mixing of fiber and matrix, but the cost of this advantage is high shear forces which may lead to fiber damage. The first process, mechanical mixing and compression molding, allows for these forces to be avoided. An additional advantage of the first process is that it produces preforms in one step. However, the lack of adequate mixing may adversely affect the overall performance. As expected, the composites formed using the second process, extrusion and injection molding, showed superior overall strength due to the adhesion and distribution of the fibers. Possibly an even more superior composite could be formed if an optimal method of fiber distribution and adhesion was introduced into the first process.

Nishino et al. (2003) [22] used kenaf fiber sheets with another processing method in an attempt to fabricate composites with better dispersion and adhesion. The kenaf fiber was bought in sheets, manufactured like paper, from a company called Itoh Co., Ltd. Japan. The sheets were dried and then soaked in a dioxane solution under vacuum. After impregnation, the composites were dried until plateau weight was reached. These samples were easily fabricated and exhibited good performance with a fiber content of approximately 70% by volume. Additionally, this study concluded that the fiber orientation plays an

important role in the final properties of the composite. Both anisotropic and quasi-isotropic composites were formed by layering kenaf sheets in different ways. From this study, kenaf has been proven to be a good reinforcement candidate for high performance natural fiber composites.

Additional research has been done to determine the effect of using the above mentioned pre-manufactured sheets of kenaf, as opposed to buying the kenaf as it is grown in nature. No information could be found on the Itoh Company. Information from another company, Vision Paper, has showed that the purchase of the 100% kenaf sheets would cost approximately \$30-\$40/kg [23], while the cost of the natural fibers themselves will only be approximately \$0.50-\$0.90/kg. The enormity of this price difference has led to the conclusion that these sheets will not be an option for the current research.

Burgueno et al. (2004) [24] attempted to establish an additional use for biocomposites as load-bearing beams and panels. They used hemp and flax fibers with an unsaturated polyester resin. By making improvements in the structural efficiency through cellular material arrangements they have allowed for natural fiber composites to be used for load-bearing components. This information may be useful for future work since this paper will show that thin layers of natural fiber composites are formable. This knowledge, in addition to the fabrication techniques and forming abilities shown in this paper may broaden the use of kenaf natural fibers.

2.2 Surface Treatments and Coupling Agents

All of the above studies have shown that natural fiber composites may be fabricated in a variety of ways to gain a variety of different properties. There is one common conclusion from each study; the most pertinent problem in making natural fiber composites is the assurance of fiber-matrix adhesion. The following is a review of surface treatments and coupling agents that have been used to strengthen the composites.

George et al. (2001) [25] attempted to solve the problem of fiber-matrix adhesion when using biocomposites. The quality of the fiber-matrix adhesion bond directly affects the transfer of stress and bond distribution throughout the interface. Natural fibers are mainly composed of cellulose, whose elementary unit, anhydro d- glucose, contains three hydroxyl (-OH) groups. These hydroxyl groups form intramolecular and intermolecular bonds, causing all vegetable fibers to be hydrophilic. The exact properties of these fibers may not be controlled because they are grown in nature, unlike the widely used glass fiber. One proposed way to make the fibers more consistent is to regenerate lost cellulose and dissolve unwanted microscopic pits or cracks in solvent. The most popular method of “fixing” the fibers is through the use of alkaline solution. The effects of this solution will be discussed later.

Another method of improving fiber matrix adhesion discussed in this work is through the use of coupling agents. The coupling agents have two functions: to react with -OH groups of the cellulose and to react with the functional groups of the matrix. In order to achieve a material with both strength and toughness, an

appropriate coupling agent must be chosen. The coupling agents will facilitate stress transfer between the fibers and the matrix. Commonly used coupling agents at the time of this study include silane, isocyanate, and titanate based compounds. Silane has been reported to improve the performance in hard wood/polymer composites. Isocyanate has been found to be reliable when used with vegetable fibers. Other modification options are further discussed in this paper, but these will not be mentioned here as this work will focus on the use of a coupling agent or an alkali solution to improve adhesion.

Feng et al. (2001) [26] studied the effects of using a compatibilizing coupling agent on kenaf-polypropylene composites. The coupling agent contains maleic anhydride, creating maleated polypropylene. The use of maleated polypropylene (MAPP) has been shown to immensely improve the properties of these composites. This study has chosen to use kenaf fiber due to the fact that kenaf flows much more easily in polypropylene than jute and flax fibers. The kenaf fibers used in this study have been chopped to approximately 10mm. The chopped fibers along with the polypropylene (PP) and MAPP, if used, were melt mixed in a kinetic mixer, followed by cooling under pressure, then granulating. The granules were then injection molded into ASTM standard test specimens. These composites were 50% by weight kenaf, and, if used, 3% by weight coupling agent (MAPP).

As expected, the systems using MAPP had consistently higher failure strains than the uncoupled systems. In contrast, the tensile modulus of the coupled systems was lower than the uncoupled systems. The tensile strengths

of coupled composites almost doubled, and the Izod impact properties were also higher for coupled samples. Once again, it has been noted that the mixing method may cause severe fiber damage, and higher strength may be achieved using another fabrication process. In conclusion, the MAPP improved both tensile and impact strengths, but there exists a strange phenomenon where the Young's Modulus was lower in the coupled composites. This occurrence was not further discussed in the study.

Mohanty et al. (2002) [27] continued researching the use of maleated polypropylene (MAPP) and polyethylene (MAPE) in comparison with the use of alkali treatment. This study fabricated composites out of chopped (5-8mm length natural fibers, including kenaf, hemp, flax, and sisal) and micron size polypropylene powder (PP). The fibers were mixed with the PP in a kitchen mixer, then compression molded at 190°C to avoid extreme shear damage during formation.

These composites contained 30-40% fiber by weight. Both bast and leaf fibers were tested, and showed a high flexural strength and Modulus of Elasticity (MOE) in the bast fibers. The kenaf composites, bast fiber, were tested with and without the use of coupling agents. The alkali (5% NaOH solution) treated fiber with MAPP (Epolene G-3003 from Eastman Chemical Company) composites showed a 31% and 63% improvement in flexural strength and MOE over the untreated. Additionally, in comparison with the MAPE-treated composites, the MAPP-treated composites showed improved flexural and tensile strength. The alkali treatment lead to fibrillation of the fibers, breaking down the bundles and

increasing the aspect ratio. Once again, the use of a coupling agent has increased the fiber properties, and, contrary to the previous study, the MOE also increased with the treatments.

Keener et al. (2004) [28] most recently compared many different coupling agents when added to agrofiber-polyolefin composites. This study has discussed the two main reasons for the success of coupling agents. The first being that maleated polyolefins (MAPO) can be readily and economically produced. The second being the excellent balance of properties which bridge the interface between hydrophilic and hydrophobic species. A variety of different coupling agents are available for use. These can be easily classified by their molecular weight and acid number. A total of six different molecular weight/acid number combination Epolene G-series maleated polyolefin coupling agents were tested in flax and jute fiber composites with a PP matrix. The control for these experiments was the 'best-to-date' maleated coupler that was tested in 2000 by ATO-DLO (Agrotechnical Research Institute).

The composites, 30% fiber by weight, were fabricated using the extrusion and injection molding processes. Three performance tests were done each on the jute and flax composites. In four of the six tests, Epolene G3015 resulted in the highest performance. This specific coupler ranks about medium molecular weight and medium acid number. It should also be noted that the coupling agents were incorporated into the composites at 1, 3, and 5% levels, with 3% appearing to be the optimum concentration. The Epolene G3015 even outperformed the 'best to date' control coupling agent. From this study, it has

been concluded that at the current time, the best coupling agent for natural fiber composites is Epolene G3015 at a concentration of 3%.

2.3 Forming Composites

Making different types of composites with properties suitable for industry has proven to be a large area of research. The next step, after proving satisfactory properties is to show the formability. In order to validate the fabrication of a new material, it must be shown to be formable and useful. There are few studies on the formability of natural fiber composites. The following will discuss findings on the formability of woodfiber composites.

Mase et al. (2004) [29] worked with recycled paperboard and began to develop a heat/pressure formable woodfiber thermoplastic composite. This new material is composed of a relatively fine polypropylene powder (20 microns) and paperboard waste. Samples were tested using 20% and 30% polypropylene with six layers of the preform pressed together. Their study has shown that the tensile modulus of this combination was increased up to twice the value of polypropylene alone. Additionally, the modulus of elasticity and ultimate tensile strength were increased, and the strain at the ultimate tensile strength was decreased. From this study it has been concluded that while this material exhibits satisfactory properties, there has been not nearly enough polypropylene added to make a formable material. There is limited resin flow during the compression forming and further processing studies will be completed in the future.

Bhattacharyya et al. (2003) [30] showed that woodfiber-polypropylene composites are indeed formable. The sheets they manufactured used pinus radiata fibers along with polypropylene powder, for a total through thickness of 1.3mm. Two types of composites were made, layered and homogeneous with polypropylene and woodfibres mixed during formation.

This study has shown a tensile modulus increase of up to 250% with a 25-30% fiber mass fraction. Several formability tests were studied, dome forming with matched die and cup drawing being most relevant. For both forming techniques the material was heated to approximately 190°C before beginning formation. This study has shown the ability to form these composites into not only 2-dimensional shapes, but also 3-dimensional hemispherical shapes. Key conclusions discovered include that any sheet not pre-heated above 160°C does not form. Additionally, slower drawing rates/strain rates leads to reduced drawability with wall tearing and wrinkling. Thinning of reinforced composites is much less than that of polypropylene. The most important parameter is the forming temperature, and too large of a blank size will lead to excessive wrinkling. The optimal forming conditions found here are at temperatures of at least 160°C, at a speed of between 200 and 500mm/min, with a 70-90mm blank, and 0.25% fiber mass fraction.

2.4 Modeling

Proving formability will show that the material is useful. In order to optimize forming conditions, an accurate way to model the behavior of the new

composite is necessary. Standard finite element analysis software has been shown to give accurate results for what are known as standard materials in the past, but must now be updated to be able to successfully predict the behavior of a random fiber orientation composite.

Yu et al. (2002) [31] worked with forming composites for some time. In this study they have shown the formability of woven fabric reinforced thermoplastics (FRT) using stamp thermo-hydroforming, as well as validated a model using explicit dynamic finite element code. The importance of this study has been the development of an updated constitutive equation that will accurately predict composite behavior based on linear elasticity and the homogenization method. In the updated constitutive equation, the microstructure of the fiber has been introduced using information such as the fiber angle. By using experimentation with in-plane simple shear, pure shear, uniaxial extension, and draping, the finite element model was validated. The material deformation was simulated using the commercial software ABAQUS and implementing a user material subroutine (VUMAT).

Yu et al. (2003) [32] continued to refine this new constitutive equation by considering shear stiffness and undulation of the woven structure. The modification has been made in order to be able to capture the wrinkling behavior more accurately. By taking into account the geometry and shear stiffness at the crossover of the warp and weft yarns, a more complete model of the behavior has been accomplished.

Zampaloni (2003) [14] wrote a thesis, which has developed this same constitutive relationship for the modeling of a random orientation composite with multiple preferred fiber orientations. He has used the model mentioned above, which focused on structured woven composites, to begin the continuum-based, non-orthogonal constitutive model for multiple preferred fiber orientations. The relevant portion of this work focused on creating a constitutive equation for a random chopped fiber glassmat reinforced thermoplastic.

The constitutive model that has been developed in this work began by studying the constitutive modeling approach developed by Dong et al. (2001) [33]. Dong developed a model for the draping of dry woven fabric. This model has demonstrated the importance of non-orthogonality on material behavior during deformation. In Zampaloni's [14] work, the updated material law with constant material properties as determined by Dong et al. [33] was developed using additional sources. The numerical data did not compare well with the experimental values in a pure shear test as determined by Dong et al. [33]. The discrepancy was attributed to the fact that some type of work hardening appeared to be occurring in the numerical simulation due to the constant material properties. From this data, it was determined that the model must again be updated to take into account varying material properties through deformation.

To begin the transformation of the constitutive model, Zampaloni [14] began by using a study by Mohammed et al. (2000) [34], which modeled dry fabrics with material properties changing with respect to the angle between the fibers. By incorporating this theory and the simple Rule of Mixtures, a new

constitutive model was created for the updated material law with varying material properties. This model was then implemented into a commercial finite element analysis code. The package ABAQUS/Explicit was chosen for this work. Using this software, the user may easily incorporate different geometries for forming as well as material properties for two preferred fiber orientation composites. The following is a list of the input parameters needed to populate the constitutive model being demonstrated in this ABAQUS VUMAT for two preferred fiber orientations:

1. Young's Modulus for fiber direction 1
2. Young's Modulus for fiber direction 2
3. Young's modulus for matrix
4. Poisson's ratio in fiber direction 1
5. Poisson's ratio in fiber direction 2
6. Poisson's ratio in the matrix
7. Shear Modulus for fiber direction 1
8. Shear Modulus for fiber direction 2
9. Shear Modulus for matrix
10. Initial fiber volume fraction
11. Original fiber 1 direction
12. Normal to original fiber 1 direction
13. Original fiber 2 direction
14. Normal to original fiber 2 direction

In addition to these 14 inputs for the VUMAT, the density of the composite and the transverse shear stiffness of the composite must also be input to run the simulation. The implementation of this model will be further discussed in Chapter 6.

Chapter 3

FABRICATION OF BIOCOMPOSITES

In the search to find the appropriate biocomposite to use for this work, there has been collaboration with the Composite Materials and Structures Center at Michigan State University. Researchers in that group have been fabricating and testing many different types of biocomposites and have expressed an interest in tests of the formability of these materials.

3.1 Fabrication of Woodfiber Composites

The first material suggested was a woodfiber-polypropylene mixture that had been fabricated by Mase et al. [29]. This woodfiber composite was made with a relatively fine powder (nominal size of 20 microns) polypropylene added to some recycled paperboard woodfiber. A traditional paper making press was used to make the composite sheets. The samples tested were made with 80% woodfiber. The composite was extremely similar to ordinary poster board at room temperature, thus the material was heated to test formability. When the material was heated in a simple oven at 170°C, burning of the cellulose occurred, ruining the material. At 150°C, the material heated more slowly and gained some flexibility and bending ability in one direction. Even with this flexibility, there was no chance of 3-dimensional formability in the current state.

To improve the woodfiber-polypropylene composite, layered samples were fabricated to increase the amount of polypropylene (PP), using compression

molding. The composite was cut into 200mm square pieces, which were compiled into 4 layers, with PP powder between each layer. These samples were placed in the press under minimal pressure at a temperature of 160°C and heated for 10 minutes. The specimens were then pressurized with 36000 lbs. for another 10 minutes. The press was then released and the samples were allowed to cool for 10 minutes before being removed. A total of four samples were fabricated using 5g, 10g, 11.25g, and 30g of PP.

After compression, these samples were all heated at 150°C and monitored for approximately one hour. For all of the samples, separation of the layers was observed. From this experiment, it can be concluded that the polypropylene powder was not able to successfully bond with the layers of the woodfiber-polypropylene to form a uniform specimen through compression. In order to fabricate a material that can be three dimensionally formed, more polypropylene must be added in the beginning of the original paper-making process.

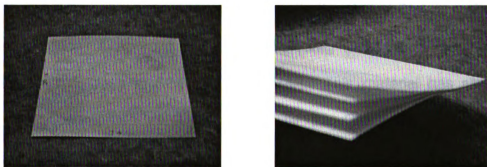


Figure 3.1 Woodfiber reinforced polypropylene composites.

At the current time, Michigan State University's Composite Materials and Structures Center is only able to fabricate this material on an extremely limited basis. This is due to the fact that the cost to rent a paper mill is approximately

\$5000/day. Due to time and financial constraints, a decision has been made to instead focus on choosing another natural material that would be more economically viable at this time and more readily available for testing.

3.2 Fabrication of Kenaf-Polypropylene Composites

Another material that has attracted interest is kenaf fiber. Kenaf is an herbaceous annual plant that is grown commercially in the United States. Kenaf may be grown in a variety of weather conditions, and it has been previously used for rope and canvas. Kenaf has been deemed extremely environmentally friendly for two main reasons. These reasons are the fact that kenaf accumulates carbon dioxide at a significantly high rate and that kenaf absorbs nitrogen and phosphorous from soil [22]. Additionally, kenaf, like most other natural fibers, demonstrates low density, high specific mechanical properties, and biodegradability [18].

Kenaf, because it is commercially grown in the United States, maintains a competitive price of approximately \$0.44-\$0.55/kg (relatively inexpensive as compared with E-glass at \$2.00-\$3.25/kg [18]). This material has also been tested and documented most extensively by the Composite Materials and Structures Center at Michigan State University. This gives access to fabrication techniques as well as additional material behavioral data.

The main problem in the fabrication of biocomposites with kenaf is the uneven fiber distribution. The kenaf fibers resemble hair and are difficult to completely separate and visually disperse evenly. The long kenaf fibers used in

the first sample were approximately 130mm. A second sample was also fabricated using these same kenaf fibers that had been chopped to an approximate length of 20mm.

These samples were both fabricated in the same way. First, polypropylene sheets were made by compression molding of a polypropylene (PP) powder named Parafax made by Bessal. The machine used for compression molding, shown in Figure 3.2, is the Carver Laboratory Press Model SP-F6030. A layer of 10g of PP powder was heated to 190°C under minimal pressure for 3 minutes. The pressure was increased to 10,000 psi for a period of 10 minutes, and then increased again to 24,000psi for another 5 minutes. The melted PP was allowed to cool to 100°C still under pressure before being released and removed immediately. This process yielded the two sheets of polypropylene that were used to make the kenaf-polypropylene composites. The thickness of the sheets was maintained at 1mm by using a steel picture frame.



Figure 3.2 Carver Laboratory Press used for compression molding

After the polypropylene sheets had been made, the kenaf fibers (30% by weight) were added by sandwiching them between the two layers of PP. This layered system was then placed inside a 1.5mm thick frame and placed into the press. These were fabricated using the same method that was used for the pure PP powder. As shown in Figures 3.3 and 3.4, both samples showed extremely poor fiber distribution.

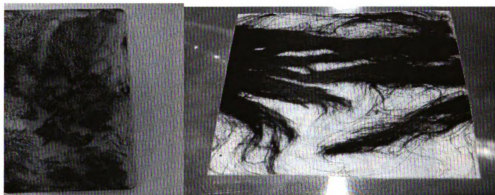


Figure 3.3 Composite fabricated by sandwiching layers with long fibers.

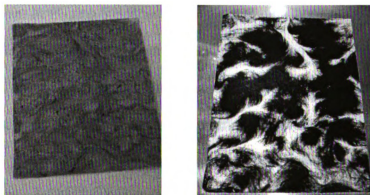


Figure 3.4 Composite fabricated by sandwiching layers with chopped fibers.

Due to the uneven fiber distribution in the sandwiched composites, a new method was tested. Instead of making layers and using polypropylene sheets, the chopped kenaf fibers were mechanically mixed with powder polypropylene in

a kitchen mixer. The PP was slowly added while mixing the fibers. This proved to be a difficult task due to the hair-like nature of the kenaf fibers. The mixer balled up the kenaf, and the denser PP fell through to the bottom of the mixer. Using gloved hands, the powder was spread more evenly though the fibers. These composites were then spread evenly into a 1.5mm thick frame and compression molded using the same method described above.

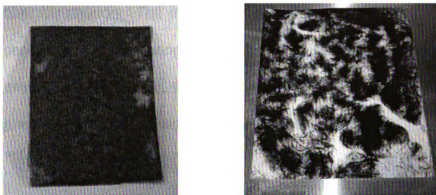


Figure 3.5 Kenaf-polypropylene composites fabricated by dry mixing.

As shown in Figure 3.5, the fibers did not distribute evenly throughout the sample. There is a tendency towards a swirling of the fibers, causing clumping and voids. The same problem has arisen, as with the sandwich composites, making it difficult to determine the even distribution of fibers due to their hair-like nature. From this series of samples, it was decided that the only suitable way to distribute the fibers would be to chop and “sift” the individual fibers in a random orientation.

The polypropylene powder was changed at this point to a Microfine Polyolefin Powder – Polypropylene. This fine powder is more easily spread and sifted. The powder was received from Equistar Chemicals, L.P. in Houston, TX.

The new "sifting" process involves sprinkling the polypropylene powder first, adding individually sifted fibers, sprinkling more polypropylene, etc. until all the desired materials were used. This method was originally tested on a small, 7" by 5.5" sample, using 20 grams of polypropylene powder and 8.5 grams of chopped kenaf fiber (approximately 30% by weight) with the same original process. From Figure 3.6, it is evident that this process has enabled the better fiber distribution. The main drawback of this method is that it is extremely time consuming. Separating the fibers must be done by hand and is a tedious process. Additionally, the kenaf that has been supplied needs to be chopped and cleaned of debris and stems while it is separated.

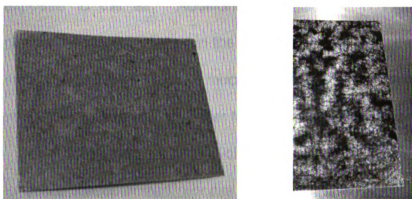


Figure 3.6 Kenaf-polypropylene composite fabricated by multiple layering of powder and fibers.

The samples that were used for the material characterization in this study needed to be 12" squares. Therefore, the powder and fiber layering method has been chosen to use for fabrication of the larger samples. A 12" by 12" square stencil with a thickness of 1.5mm will be used to determine the size and thickness of the samples. Problems occurred using the above-described method to fabricate the larger samples.

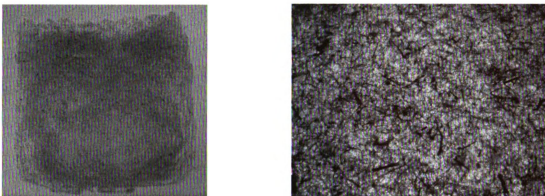


Figure 3.7 Twelve inch kenaf-polypropylene composite fabricated by multiple layering of powder and fibers.

These samples did not allow for the polypropylene to fully engulf the fibers. The surfaces of these samples were rough and some fibers were exposed to the air. Additionally, as shown in Figure 3.7, not all of the polypropylene was melted in the process. It has been determined that due to the enlargement of the sample, much more material had to be added. Also, a larger size press was needed in order to evenly heat the material.

Further analysis of the volume fractions led to the conclusion that, in order to utilize the optimized process for the larger sample, six times the amount of each of the materials must be used. In order to ensure even heating, the Tetrahedron Smart Press was used to make the larger samples. As shown in Figure 3.8, this press is similar to the Carver Laboratory Press. The differences between the presses are that the Tetrahedron is digitally controlled and that the Tetrahedron has compression area of 14" square, while the Carver is manually controlled and only has a 12" square area. This additional 2" gives the samples the ability to heat uniformly all the way to the edges. By incorporating these changes, usable kenaf-polypropylene samples have been fabricated.



Figure 3.8 Tetrahedron Smart Press used for compression molding

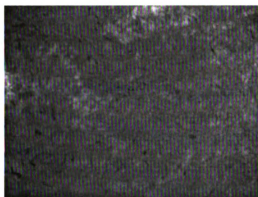
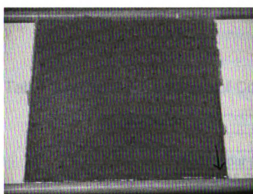


Figure 3.9 Final kenaf-polypropylene biocomposite with 30% fiber by weight.

In order to further improve the composite samples, both the kenaf fibers and the polypropylene powder were altered. In order to remove any excess moisture, the kenaf fibers are now baked in a vacuum oven at 30°C for at least four hours prior to fabricating. The decrease in moisture content decreases the weight of the fiber; therefore, more fiber reinforcement will be added in the 30%

by weight composite. In addition, withdrawing the moisture allows the fibers to be chopped and spread more easily.

The polypropylene was modified by the addition of a coupling agent to increase fiber to matrix adhesion. The chosen coupling agent is Epolene Wax G3015 (MAPP) in powder form from the Eastman Chemical Company from Kingsport, Tennessee. As discussed earlier, this coupling agent has been previously used in a study of maleated polyolefin coupling agents for agrofiber composites and has been proven to increase flexural and tensile strengths by more than 60% [28]. According to this and other studies [26,27], the optimal amount of coupling agent is 3% for a range of different fiber amounts. In order to accommodate the coupling agent, 3% of the polypropylene powder was replaced with the Epolene Wax G3015.

Table 3.1 Optimal Quantities of Composite Components

Material	Amount by weight (g)**
Kenaf	37.6
Polypropylene Powder (PP)	82.2
Epolene Wax G-3015 P (MAPP)	3.8

****Scale these quantities for every 100,000mm³ volume**

In summary, the optimized process for the fabrication of strong, useful, manufacturable kenaf-polypropylene composites can be seen in Figure 3.10. Additionally, the amounts of each material per unit volume may be found in Table 3.1. These amounts have been tested in fabrication of picture frame volumes between 22,580mm³ and 278,700mm³. For this range of volumes, the following process has proven to be optimal.

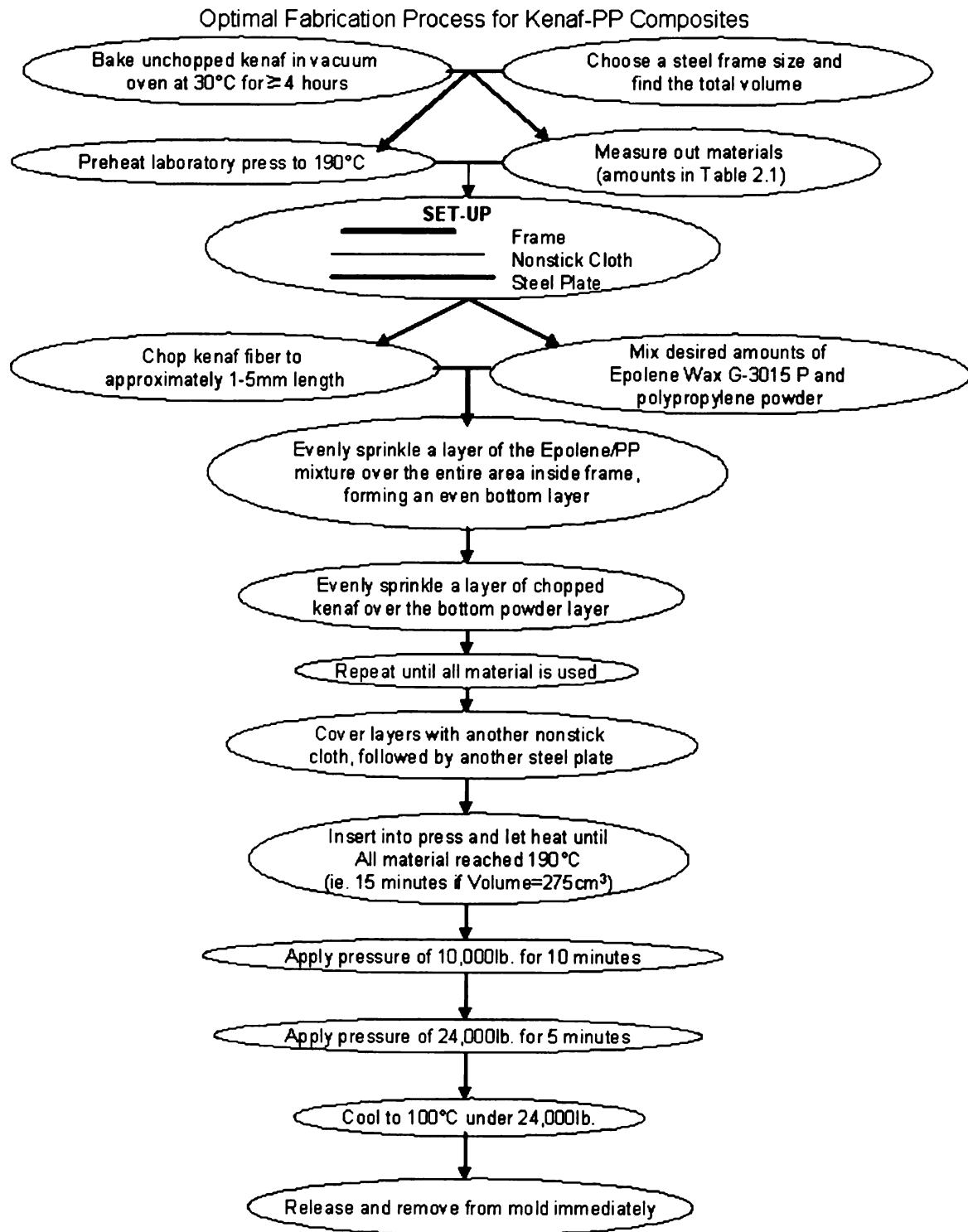


Figure 3.10 Flow chart of optimal fabrication process

Chapter 4

CHARACTERIZATION OF THE MATERIAL PROPERTIES

The kenaf-polypropylene-Epolene G3015 composites must now be characterized. The standard test methods may not be used for this material because the natural fibers give different material characteristics in different directions. A test method called Squeeze Flow Testing was previously used by Michael Zampaloni to characterize a glassmat composite [14]. The same technique will be used to begin characterization of these natural fiber composites by identifying the principle directions of the material. Two preferred fiber orientations will be chosen in order to accumulate the data to populate the constitutive model used for simulation.

4.1 Squeeze Flow Testing

During squeeze flow testing, the material is heated to the matrix melt temperature (190°C). Then, it is pressurized in order to let the natural fibers flow to preferred fiber orientations. The squeeze flow tests were done using both the Carver Laboratory Press and the Tetrahedron Smart Press in order to save time. The same procedure was used to make 24 samples.

Each sample was a 3" diameter circle, which was cut out of a 12" square preform with an original thickness of 3mm. Care was taken to observe the zero direction and exact center of each sample. The integrity of this direction was upheld by the fact that the frame used to fabricate the composites was oriented

the same for each 12" square preform. Prior to cutting out the 3" diameter circles the same zero direction was marked on each sample. Additionally, that zero direction was marked again on each sample immediately following compression molding.

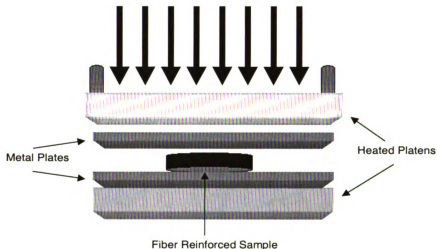


Figure 4.1 Schematic of Squeeze Flow Test experimental setup

Shown above in Figure 4.1 is a schematic of the Squeeze Flow experimental set-up. Prior to testing, the presses were heated to 190°C. The squeeze flow samples were placed between metal plates and then placed into the presses. The heated platens were closed just enough to touch each sample with slight pressure. The samples were then left to heat up evenly to 190°C for forty minutes in this position. After forty minutes, the platens were compressed to a pressure of 12,000 lbs. for sixty seconds. Following pressurization, the samples were immediately removed from the mold and left to cool between the metal plates in air.

After all 24 samples were pressed, they were labeled in increments of 10 degrees going completely around the sample starting with the zero direction, as shown in Figure 4.2. This was done so that measurements could be taken at each increment to determine in which directions the fibers tended to spread the most or least.

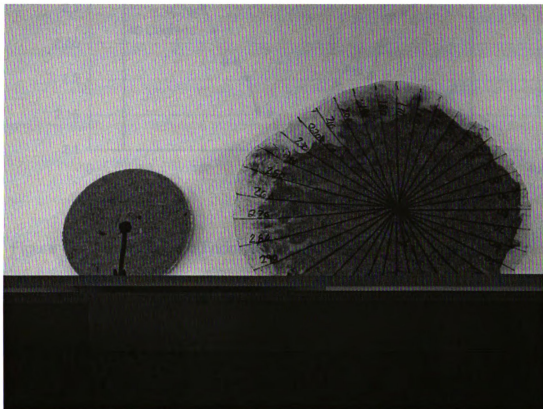


Figure 4.2 Squeeze flow test sample before (right) and after (left) compression

After testing, measurements on all the samples needed to be taken and organized. The distance to the edge was measured from the original center point at each 10° increment and then divided by the original distance to the edge to normalize the data. An average of all 24 samples was taken, which is shown in Figure 4.3.

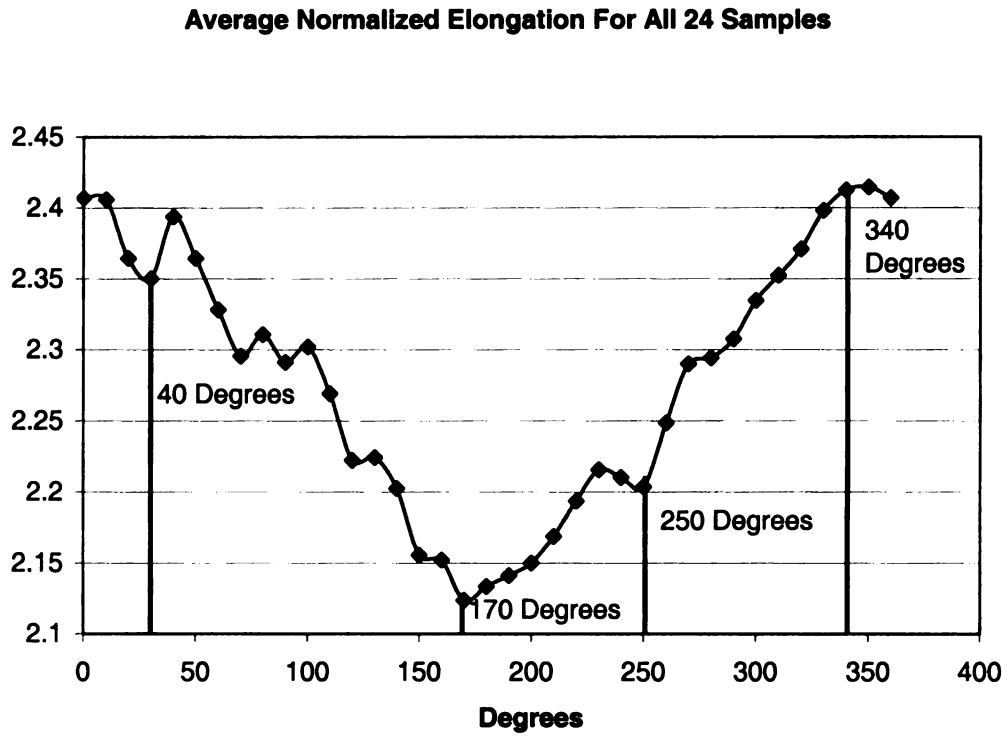
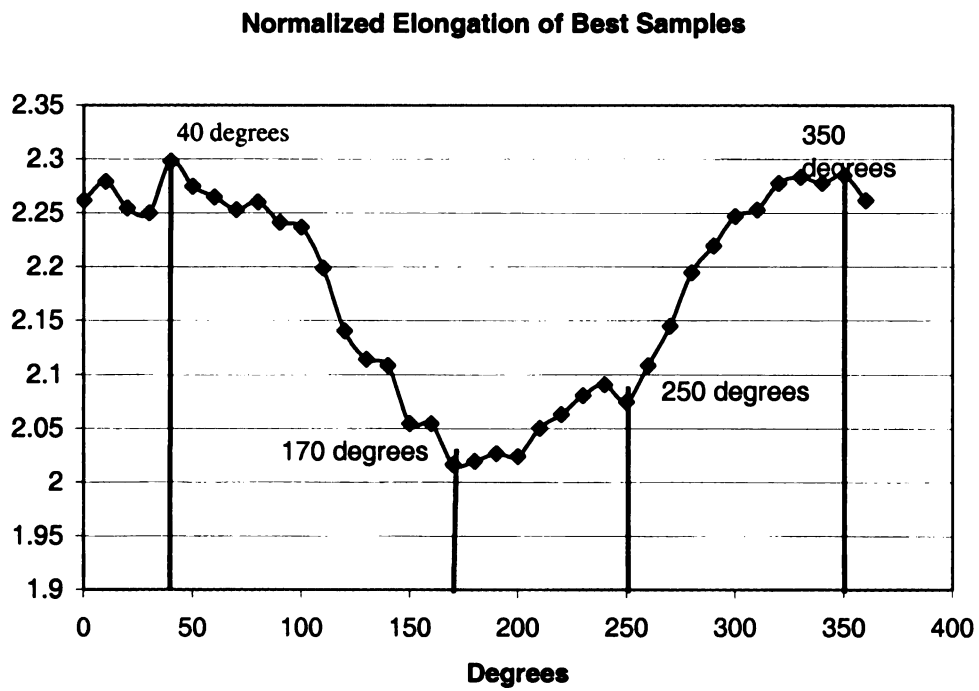


Figure 4.3 Plot of averaged normalized squeeze flow data for all 24 samples



To choose preferred fiber orientations, the goal is to chart all the data, and determine where there are noticeable peaks or valleys in the graph. The initial four angles chosen were 40, 170, 230, and 340 degrees. In order to make sure these results were as accurate as possible; a few of the samples (i.e. 2, 3, 9, 10, 17, and 22) were removed due to the fiber clumping during testing. Figure 4.4 shows that the prevalent angles when excluding possible incorrect data are at 40, 170, 250, and 350 degrees. While similar to the original data, the only two angles that exactly matched in both plots were 40° and 170°. Additionally, these two values appear to be the absolute maximum and minimum values. Therefore, 40° and 170° were chosen as the two preferred fiber orientations. These two preferred fiber orientations were used to characterize the material properties and populate the numerical model.

4.2 Tensile and Flexural Testing

These tests are static tests performed on the composites, as well as polypropylene and Epolene G3015 (PP/MAPP) sheets at room temperature. The results are immensely dependent on the fiber orientation with respect to the loading axis. For this reason, as determined in the previous section, the samples used for these tests have been cut out of 12" preforms at the specified preferred fiber angles of 40° and 170°.

The tensile tests have been completed twice for each sample. In the first set of experiments, the samples were exerted to tension in the longitudinal direction

until break to determine the Young's Modulus and the tensile strength. In the second set of tests, the samples were only tested to a strain of 0.8% extension. This was done in order to protect the strain gages from damage while determining Poisson's ratio of the composites using both axial and transverse strain. In addition to the tensile tests, the flexural test loaded the composites with a mixture of tension, compression, and shear forces to determine more information about the performance.

All of these tests were performed on the UTS Machine, Model SFM 20 of United Calibration Corporation, with the twin screw loaded frame shown in Figure 4.5. Originally, sampling coupons were cut to a length of 9" and a uniform width of 1" prior to testing (ASTM Standard D3039). Two trials with these samples proved to break near the grips, giving inconclusive results. It was then determined that the dogbone tensile coupon shapes detailed in ASTM Standard D638 would need to be used in order to obtain accurate results. Table 4.1 gives test conditions for each characterization test, and Table 4.2 gives a summary of the test results for PP/MAPP, kenaf-PP/MAPP at 40°, and kenaf-PP/MAPP at 170°.

Typical stress-strain plots have been supplied for each of the three types of samples. These plots were used for the elastic Young's Modulus (E) calculation. The value of E is determined by taking the slope of the initial linear portion of the stress-strain plot. Additionally, typical strain-load plots, as detailed in ASTM Standard D638, are shown to demonstrate the Poisson's Ratio calculation. The

value of ν is given by taking the negative of the ratio of the slope of the Transverse Strain divided by the Axial Strain.

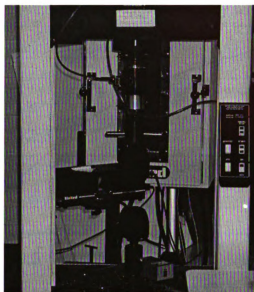


Figure 4.5 UTS Machine

Table 4.1 Conditions for Tensile and Flexural Tests

	Tensile Test to Break	Tensile Test for ν	Flexural Test
ASTM	D638	D638	D790
Temperature	30°C	30°C	30°C
Strain Recorder	Laser Extensometer	Biaxial Strain Gage	Strain Gage
Loadcell Capacity	1000 lb.	1000 lb.	1000 lb.
Test Speed	0.2 in./min.	0.2 in./min.	0.06 in./min.
Specimen Dimensions	Gage length – 2 in. Width – 0.5 in. Thickness – 0.12 in.	Gage length – 2 in. Width – 0.5 in. Thickness – .12 in	Span – 2 in. Width – 0.5 in. Thickness – .12 in

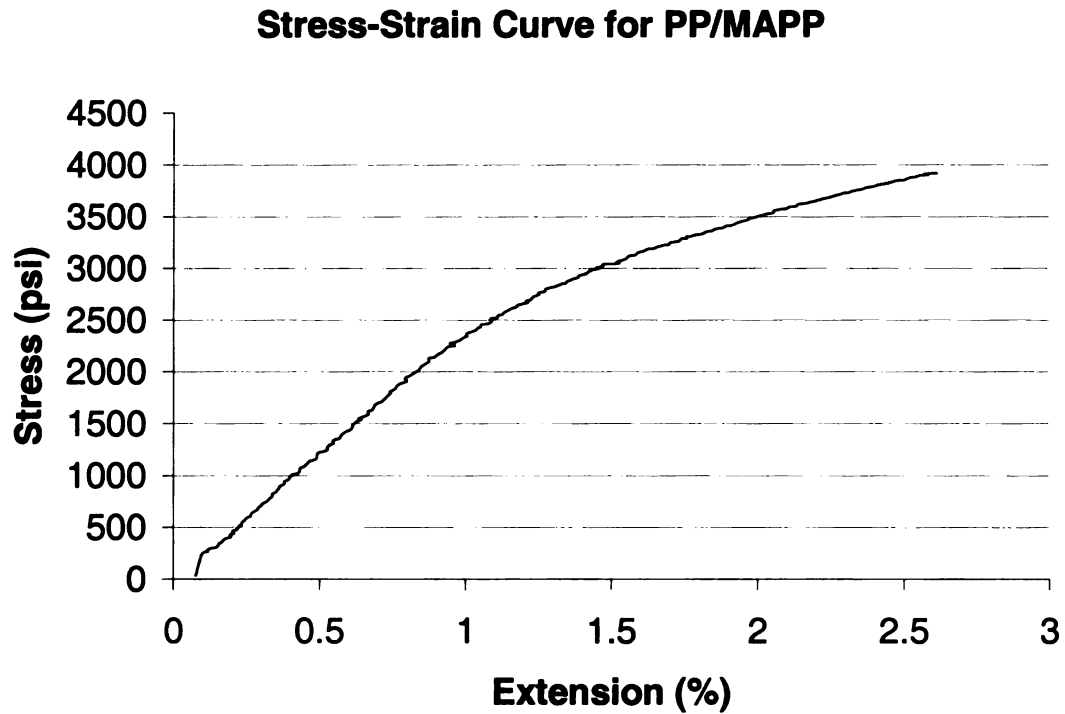


Figure 4.6 Stress-strain curve for PP with 3% MAPP

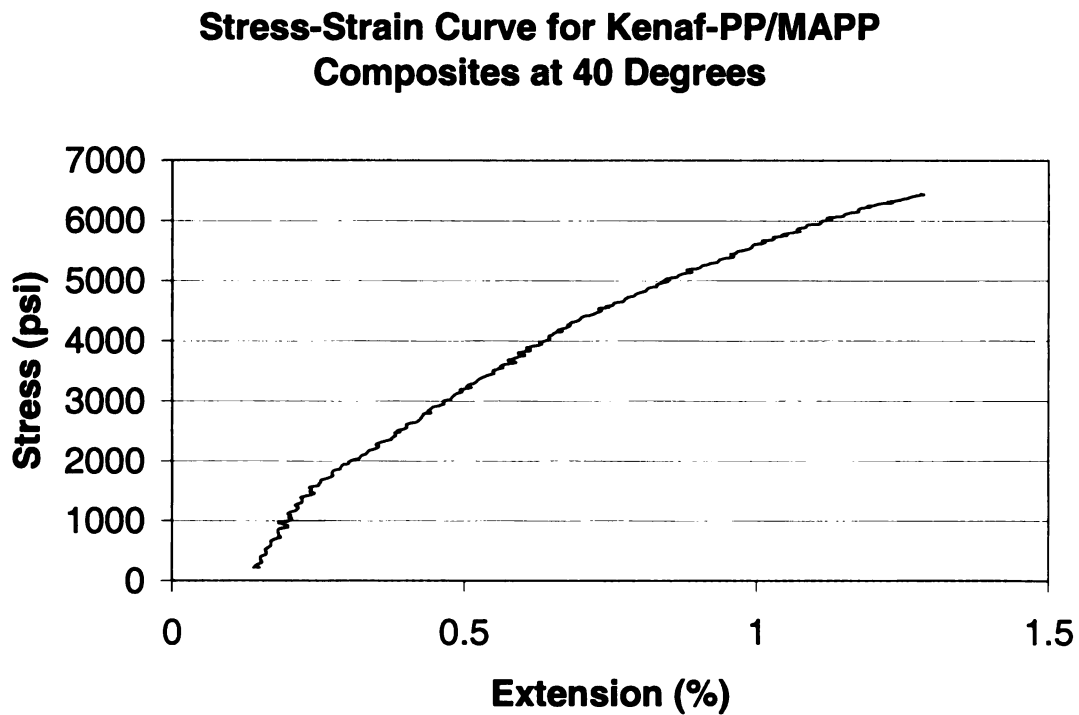


Figure 4.7 Stress-strain curve for 30% kenaf, 67% PP, and 3% MAPP at 40°

Stress-Strain Curve for Kenaf-PP/MAPP Composites at 170 Degrees

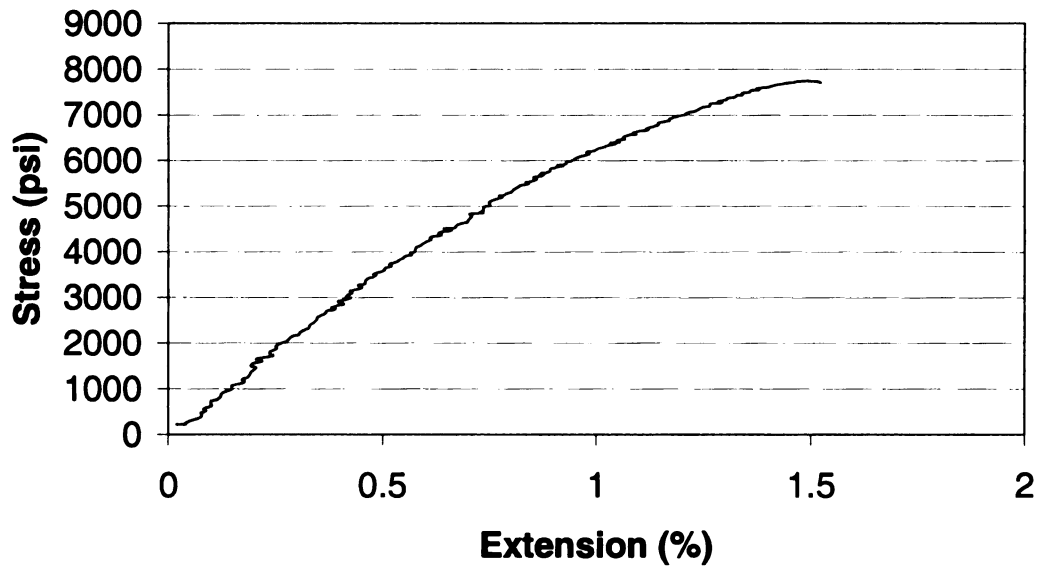


Figure 4.8 Stress-strain curve for 30% kenaf, 67% PP, and 3% MAPP at 170°

Strain-Applied Load Curves for Kenaf-PP/MAPP Composites at 40 Degrees

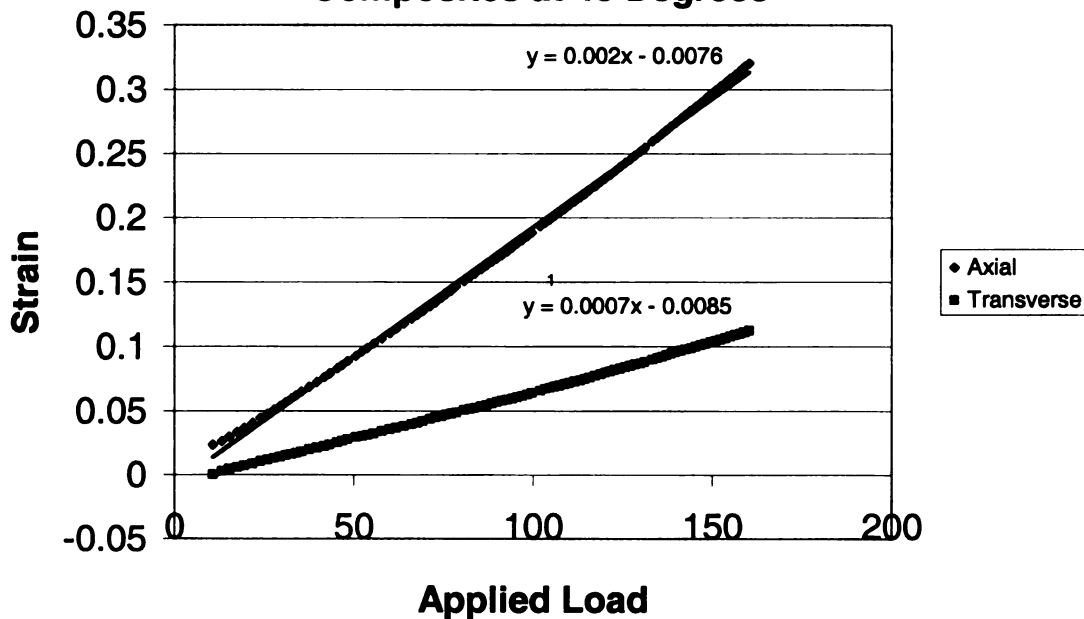


Figure 4.9 Strain-load curve for 30% kenaf, 67% PP, and 3% MAPP at 40°

Strain-Applied Load Curves for Kenaf-PP/MAPP Composites at 170 Degrees

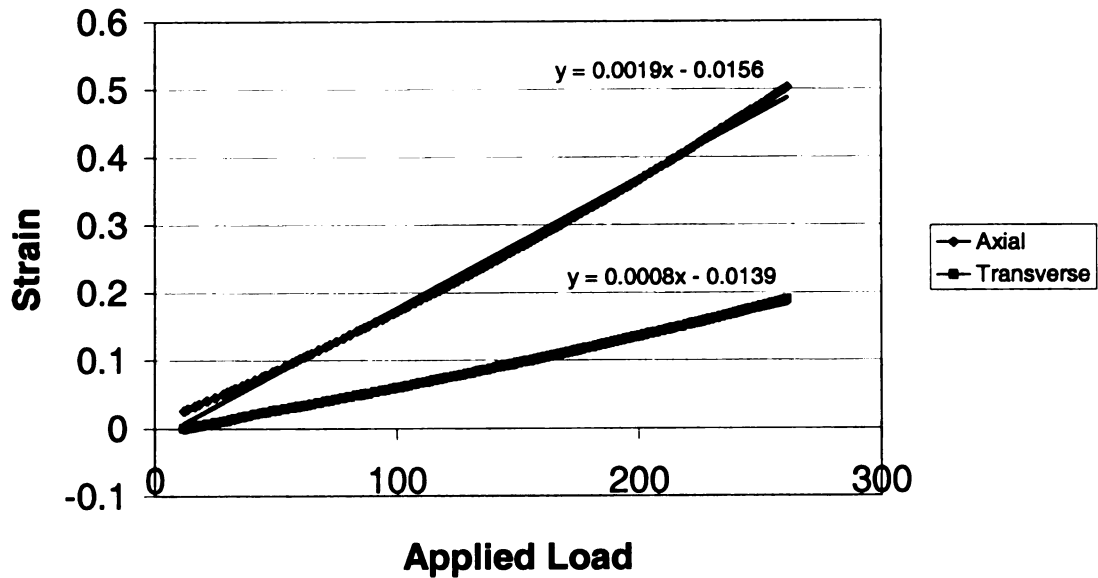


Figure 4.10 Strain-load curve for 30% kenaf, 67% PP, and 3% MAPP at 170°

Table 4.2 Mechanical Properties from Tensile and Flexural Tests

	Elastic Modulus (MPa)	Poisson's Ratio	Flexural Modulus (MPa)
PP/MAPP	1,797	-----	-----
Kenaf-PP/MAPP 40°	4,153	0.35	3,632
Kenaf-PP/MAPP 170°	4,835	0.42	4,035

In order to evaluate the effectiveness of the kenaf-PP composites, they have been compared to other natural fiber composites. Figures 4.11 and 4.12 show a comparison of the kenaf-polypropylene composites made in this study to other compression molded natural fiber-polypropylene composites with

40% wt. fiber. These composites were fabricated using polypropylene films, with natural fiber layers randomly spread between them [19].

The kenaf-polypropylene composites fabricated using the optimal sifting process used in this study outperformed all of the other fibers, except hemp. The fact that the properties of kenaf-PP composites improved by introducing the powder PP and fiber “sifting” technique proves that better matrix fiber adhesion has been achieved. The matrix was able to transfer the loads applied to the stiff fibers, using the full capabilities of the composite material. Additionally, the kenaf-PP composites fabricated in this study were composed of only 30% wt. fiber. Nevertheless, the kenaf composites had a Tensile Strength of within 5 MPa of the hemp-PP composite. The tensile strength of the hemp fiber alone is 550-900 MPa while kenaf ranges from only 284-800 MPa [2,19].

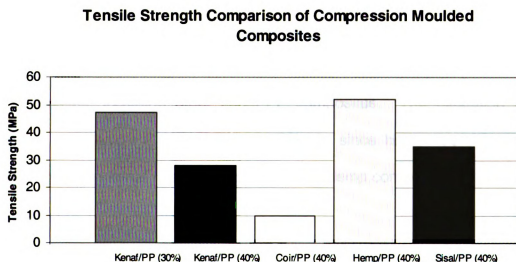


Figure 4.11 Comparison of tensile strength of kenaf/PP-MAPP composites to other natural fiber composites

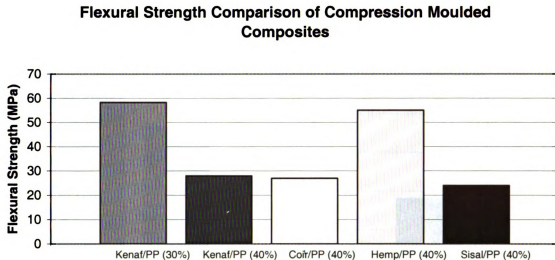


Figure 4.12 Comparison of flexural strength of kenaf/PP-MAPP composites to other natural fiber composites

The flexural strength of the sifted kenaf-PP composites was also compared with previous results from other compression molding studies [18]. This has shown that the sifting process, along with the MAPP coupling agent, has produced nearly double the flexural strength of some other natural fiber composites, including other kenaf-PP composites. The exception was once again the hemp-PP composites. Although, since hemp fibers in general are stronger than kenaf fibers, it is believed that hemp composites produced with the sifting

With the elastic modulus data calculated from testing, it is also possible to compare the benefits of using this kenaf composite over other natural fibers as well as E-glass. Figures 4.13 and 4.14 illustrate that these kenaf-PP composites have a higher Modulus/Cost and a higher Specific Modulus than sisal, coir, and E-glass.

Comparison of Specific Modulus for Various Fibers

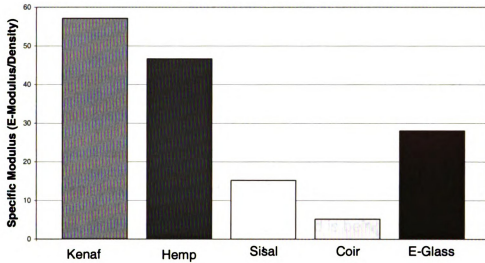


Figure 4.13 Comparison of Specific Modulus of various fibers

Comparison of Modulus Per Cost for Various Fibers

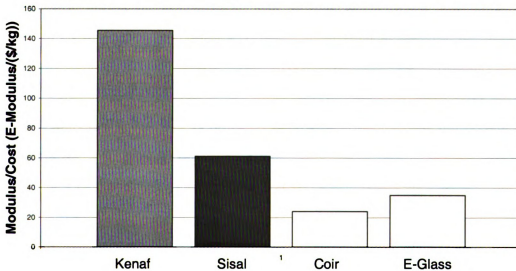


Figure 4.14 Comparison of Modulus per Cost for various fibers

Chapter 5

EXPERIMENTAL WORK

The optimally fabricated and characterized kenaf-polypropylene with maleated polypropylene (PP/MAPP) composites were next tested for formability. The process of stamp thermoforming has been chosen for this work. This newer process has been developed by the research team under Dr. Farhang Pourboghrat, at Michigan State University, and is being constantly improved.

5.1 Experimental Apparatus

The apparatus used for the experiments in this work is the in-house stamp thermo-hydroforming press originally built by Interlaken Technology Corporation, Eden Prairie, Minnesota. The press is a double action servo press, Figure 5.1, where the clamping mechanism and punch mechanism are able to move independently of one another. The die has been re-designed by Nader Abedrabbo, Ph.D. student at Michigan State University, to allow room for material wrinkling. Figure 5.2 shows a schematic of the stamp thermoforming process, and Figure 5.3 shows the actual experimental press with the wrinkling die installed.

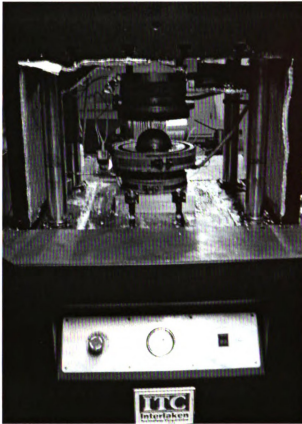


Figure 5.1 Double action servo press 75 manufactured by Interlaken Technology Corporation [13]

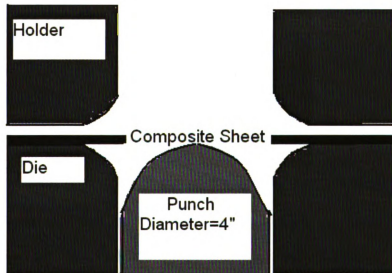


Figure 5.2 Schematic of stamp thermoforming set-up

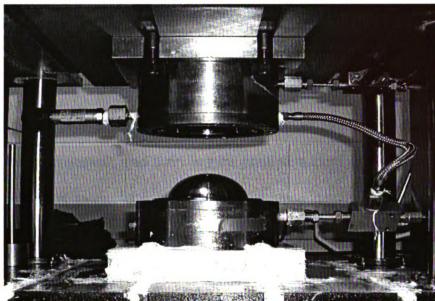


Figure 5.3 Modified Interlaken press for stamp thermoforming

Not shown in Figure 5.3, are the heating bands that have been added around the upper and lower dies. For this preliminary experimentation the upper heating bands will not be necessary, as there will be no fluid in the upper chamber. The option of adding fluid into the upper chamber is used for stamp thermo-hydroforming. Since this is only a preliminary experimentation of stamp thermoforming, this study will not include the fluid pressure.

5.2 Thermoforming Results

In order to form usable parts out of the kenaf-polypropylene preforms, they must be heated to the forming, or glass transition, temperature of the polypropylene. At room temperature, thermoplastic materials are extremely brittle and will simply fail when stamped. The forming temperature chosen for this work is the temperature at which the composite becomes malleable and

easily shaped. The glass transition temperature of the polypropylene is 190°C, which has been used for fabrication and fiber mixing. This temperature is extremely close to the burning temperature of the fiber; therefore, extra care must be taken to ensure accurate and frequent temperature checks.

Originally, the preforms were heated at 190°C in a conventional toaster oven for 20 minutes, and then tested against a cool die. The ambient air cooled the preforms below the forming temperature before stamping could be executed. The cooling resulted in large breakage and tearing during forming. This is shown in Figure 5.4. While moving the preform from the oven to the die the sample loses some heat, which affects its formability. However, to prevent this problem, preforms cannot be heated longer or to higher temperatures without burning and thermal degradation of the material. In order to help maintain the elevated temperature needed for forming, the outer ring heating bands on the bottom die were utilized. These heating bands allowed the outside of the die to heat up to close to 190°C, giving a top surface temperature of around 180°C.



Figure 5.4 Kenaf-PP/MAPP composite formed in ambient conditions

In addition to the problem of maintaining forming temperature, the heated composites were becoming “sticky”, making transport between the oven and the press difficult. To remedy this problem, a circular metal plate has been cut to exactly 7” in diameter, with a 4” hole placed in the center for the punch to move through. Adding a layer of non-stick Teflon paper to the top of this plate was able to solve both the sticking problem and eliminate transport difficulty. Additionally, the metal plate is heated and helps to keep the temperature of the composite close to 190°C.

Many preforms were tested at a variety of different forming conditions using the above mentioned heat retention technique. The forming parameters listed in Table 5.1 are the optimum forming parameters for the kenaf-polypropylene-Epolene composites with a hemispherical punch. Using preforms of this size and forming conditions stated, the formed parts exhibited similar wrinkling behavior.

Table 5.1 Thermoforming Parameters

Preform Diameter (in.)	Preform Thickness (in.)	Preform Heating Time (minutes)	Die Heat Temperature (°C)	Draw Depth (in.)	Gap between Dies (in.)
6.5	0.118	15	165	4	0.6

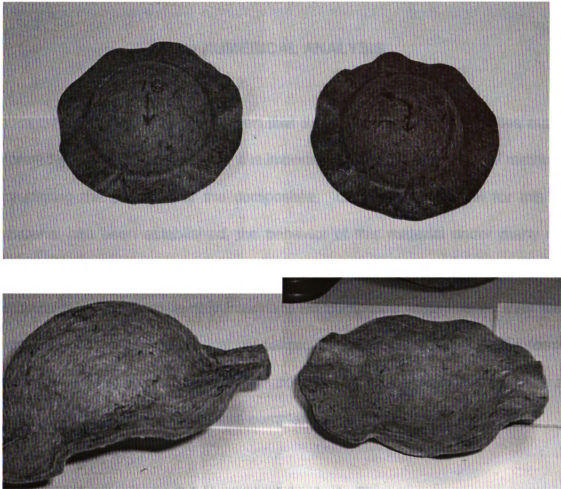


Figure 5.5 Typical thermoformed kenaf-MAPP composite

Notice that there are 6 distinct wrinkles in both samples, with the two distinct “crinkles” showing in the same pattern on each. The goal will now be to capture this behavior using the commercial finite element code ABAQUS/Explicit.

Chapter 6

NUMERICAL ANALYSIS

Now that it has been proven that these natural fiber composites may be formed into hemispherical cups, it is important to develop a numerical method for predicting the behavior of the composites. Once a valid model for this new material has been established, the behavior of this material under many more conditions may be studied, as well as optimization performed to meet product standards. This is extremely important for composite materials as they easily wrinkle and buckle. Numerical model proven to accurately predict the forming and wrinkling of the kenaf-PP/MAPP composites will be used to save time and money in the design of new, more complex dies and punches.

6.1 Numerical Analysis Theory

In order to accurately predict the behavior of the material during the stamping process, finite element analysis (FEA) will be used. Commercial codes are extremely valuable in predicting how parts will react during conditions specified such as pressure and holding forces. Composite materials are difficult to model, as they are heavily dependent on the relationship of the fibers and the matrix. As discussed earlier, Michael Zampaloni [14] developed a VUMAT to be used with the commercial software ABAQUS that can take into account composite materials with non-orthogonal properties. The VUMAT is a modified

linear elasticity model based on the well known Hooke's Law. The inputs required for this updated constitutive model were found through experimentation. These values are listed in Table 4.2.

6.2 Properties for the Numerical Model

The data in Table 4.2 can be used to populate the constitutive model. The parameters that are yet to be known are the Shear Modulus in each fiber direction (G), the transverse shear stiffness of the composite, and the initial fiber volume fraction of the composite.

There is no test available that may be used to determine G experimentally; therefore, an elementary equation will be used from a Continuum Mechanics textbook [34]. For isotropic materials the following relation may be used:

$$G = \frac{E}{2(1 + \nu)}$$

This material is obviously not isotropic, as evidenced during squeeze flow testing, but sensitivity analysis of this parameter has been completed and will be discussed later.

The transverse shear stiffness was computed using the ABAQUS Analysis User's Manual [36]. The data will be used in ABAQUS/Explicit with shell elements. The value of the transverse shear stiffness is computed for small-strain shell elements using the effective shear modulus. Due to the fact that no effective shear modulus data was available, the transverse shear stiffness was calculated simply using the shear modulus calculated above. This value also has

been tested for sensitivity by numerical simulation. The results will be discussed later in this chapter.

The initial fiber volume fraction is the final property needed to complete the model. The composites were fabricated with 30% kenaf fiber by weight; therefore, the density must be used in order to calculate the volume fraction. The density of the PP/MAPP has been assumed to be 0.909g/cm^3 based on the Material Data Sheet provided by Equistar Chemicals [37]. The density of the kenaf fiber is an uncertain factor. Several sources [38-40] have documented the density of kenaf fiber to be 1.4g/cm^3 . This value was evaluated using a simple water test of the fiber. If the correct density of the fiber was 1.4 g/cm^3 , then the fiber would sink when placed in water. Surprisingly, the fiber did not sink, but instead floated in the water for over 1 hour.

Additional research was then performed to try to obtain the correct density of kenaf fiber. Several studies [41-45] listed the density of kenaf between 0.25 and 0.44g/cm^3 . The reason for the differences in these values is due to the difference in environmental conditions. It has previously been shown that the kenaf fiber does vary depending on growing environment [12]. Selecting a density of 0.3g/cm^3 for the kenaf would give an initial fiber volume fraction of approximately 0.5. This value will be used first, but sensitivity analysis of the initial fiber volume fraction must also be completed in order to validate the model.

Table 6.1 Input Parameters for VUMAT

Property	Input Value
1. Young's Modulus for 40°	4.15E9 Pa
2. Young's Modulus for 170°	4.84E9 Pa
3. Young's Modulus for Matrix	1.50E9 Pa
4. Poisson's Ratio for 40°	0.35
5. Poisson's Ratio for 170°	0.42
6. Poisson's Ratio for Matrix	0.1
7. Shear Modulus for 40°	1.23E9 Pa
8. Shear Modulus for 170°	1.43E9 Pa
9. Shear Modulus for Matrix	0.20E6 Pa
10. Fiber Volume Fraction	0.5
11. Original Fiber 1 Direction (40°)	1.0
12. Normal to Fiber 1 Direction	0.839
13. Original Fiber 2 Direction (170°)	-1.0
14. Normal to Fiber 2 Direction	0.176

Table 6.2 Additional Input Parameters

Property	Input Value
Density of Composite	993 kg/m ³
Transverse Shear Stiffness	1.23E6 Pa
Material Thickness	0.002 m

The VUMAT is implemented into an ABAQUS input file, originally written by Michael Zampaloni, that has been modified for the new kenaf-PP/MAPP composites with two preferred fiber orientations of 40° and 170°. Since the material is not isotropic, symmetry may not be used and a full model is necessary to fully capture the behavior of the composite. The punch, blank holder, and die are simplified by assuming that they are rigid shell elements, not able to deform. The blank holder and die are constrained to absolutely not move, while the punch may only move in the z-direction. Figure 6.1 shows the undeformed geometry created by the ABAQUS input file.

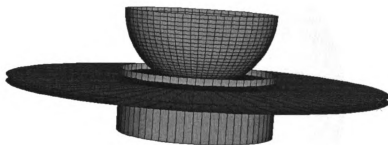


Figure 6.1 Undeformed model of the thermoforming process using ABAQUS

Although it is difficult to see the blank (preform) in this view, Figure 6.1 gives an adequate representation of all of the rigid elements in the model. The small gap between the blank holder and the die remains constant through forming to allow for wrinkling, as is done in the experimentation. The mesh of the blank that was originally used has been modified. As shown in Figure 6.2, the number of elements at the center of the part has been decreased, while the same number of elements was used in the flange area. This change has been made in order to decrease the total number of elements and the total simulation time.

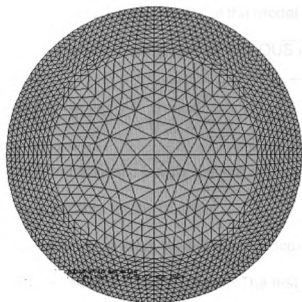


Figure 6.2 Undeformed mesh of the blank in ABAQUS

The total simulation time has proven to be an important factor in this analysis. Due to the complex nature of the composite behavior, extremely long run times have been experienced using the parameters given in Tables 6.1 and 6.2. The simulation is set to run for a total of 20 steps, but using the correct parameters, this simulation was computing at a rate of approximately 4 days per step. This is an unacceptable amount of time, not only for this work, but also for future work. The expense of taking that much time to run is unrealistic in industry.

The simulation time is determined by the time step Δt . In order to obtain an economical solution to the problem, the time step must be increased. The problem with increasing the time step is that this may lead to a state of dynamic

equilibrium with dominant inertial forces. It is important to retain quasi-static analysis conditions in order to prove the validity of the model. The time step used in ABAQUS/Explicit analysis is computed by ABAQUS using the equation

$$\Delta t \leq \min(L^{el} \sqrt{\frac{\rho}{\lambda + 2\mu}})$$

where L^{el} is the element characteristic length, ρ is the density of the material, and λ and μ are the Lamé's constants for the material.

In order to increase the time step, the ABAQUS Documentation [36] suggests using one of a possible of three methods. The first would be to simply scale the density of the entire blank material. The other two options are variable and fixed mass scaling. Scaling the density of the entire blank would change each element by simply scaling from a density of 993 kg/m³ to multiples such as $\rho \cdot E2$ kg/m³, $\rho \cdot E4$ kg/m³, or $\rho \cdot E6$ kg/m³. The fixed mass scaling has basically the same function of scaling the density. When choosing the fixed mass scaling option, a time step is selected, and the mass/density of all elements in the blank are scaled in order to make the time step equation hold.

The final option that may be used is the variable mass scaling option. In this option a desired element-by-element stable time step is chosen. The elements are checked at a specified frequency, and those elements having a time scale not equal to the specified time scale are mass scaled to increase the time step. Care must be taken when using these methods to insure that the process remains quasi-static. One equation that must always be satisfied throughout the simulation is the following

$$\frac{KineticEnergy}{InternalEnergy} \leq 10\%$$

Plots of both the kinetic energy and internal energy have been selected as output parameters in order to monitor this relationship and maintain a valid solution.

6.3 Mass/Density Scaling Sensitivity Analysis

Several simulations have been run in an attempt to discover what effects scaling the mass/density of the composite would have. The techniques of simple density scaling and variable mass scaling have both been tested and analyzed. Several simulations have proven to show that variable mass scaling produces the same results as simple density scaling. This is the expected result due to the fact that the density is directly related to both the time step and the mass. The actual density of the kenaf-PP/MAPP composite is 993 kg/m³. When comparing simulations using $\rho \times 2$ kg/m³, $\rho \times 4$ kg/m³, and $\rho \times 6$ kg/m³ there is minimal difference in results. The most significant change is the increase in both internal and kinetic energy as the density is scaled up.

Table 6.3 Density Scaling Sensitivity Analysis Results

Density (kg/m ³)	Number of Wrinkles	Maximum Internal Energy (Joules)	Maximum Kinetic Energy (Joules)
993	18	8 E5	0.9
993 E2	14	120 E6	2.5
993 E4	14	120 E8	2.2
993 E6	15	120 E10	4.5

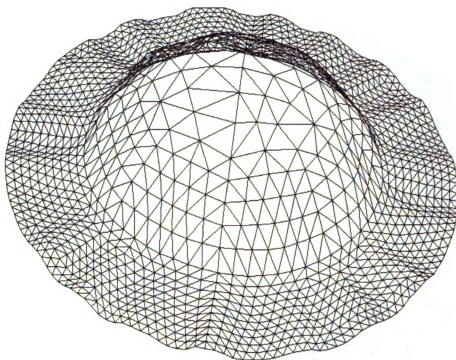


Figure 6.3 Numerical simulation results with density of 993 kg/m^3

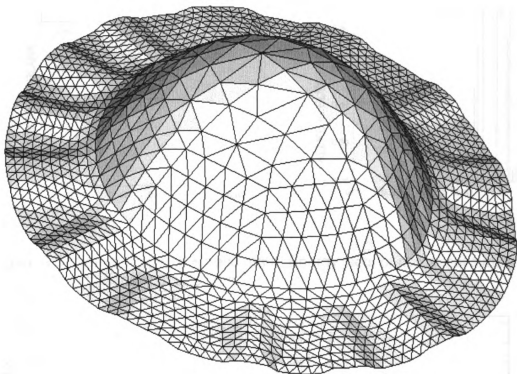


Figure 6.4 Numerical simulation results with density of $993\text{E}2 \text{ kg/m}^3$

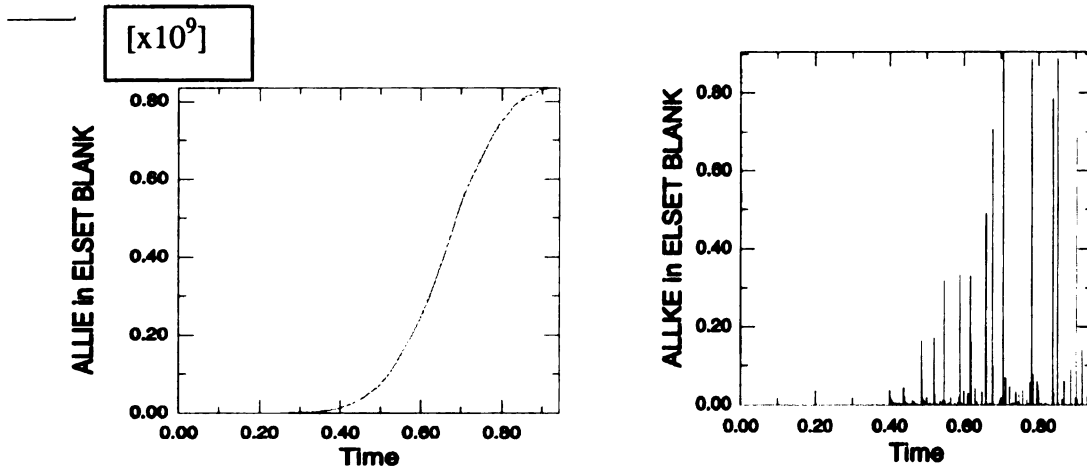


Figure 6.5 Internal (left) and Kinetic (right) Energy plots of numerical simulation with density of 993 kg/m^3

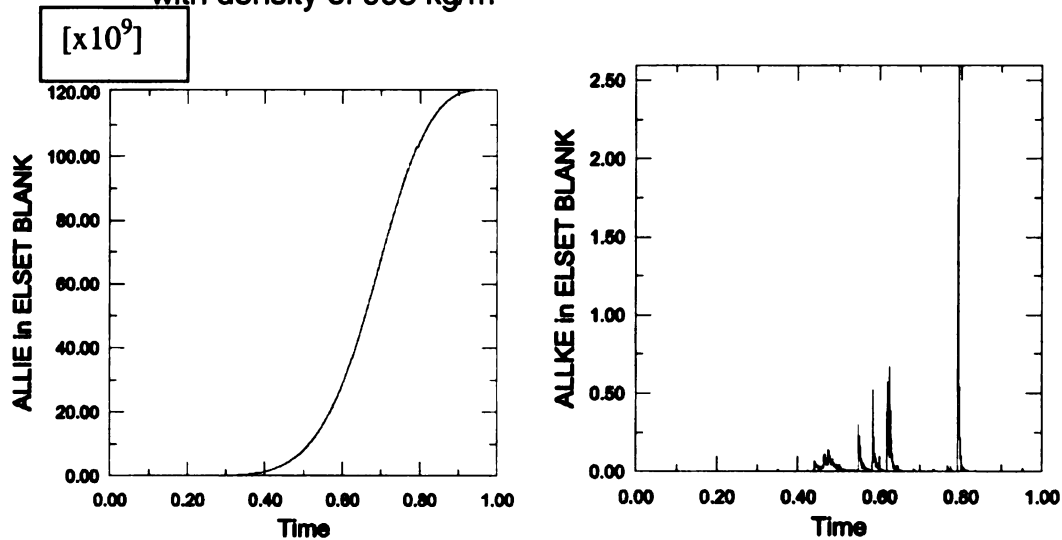


Figure 6.6 Internal (left) and Kinetic (right) Energy plots of numerical simulation with density of $993\text{E}2 \text{ kg/m}^3$

The results shown above for the $993\text{E}2 \text{ kg/m}^3$ density are typical of both of the other increased density simulations. It may be noted that the ending internal energy increases with the density, but it follows the same curve qualitatively. The increase in internal energy is expected due to the increase in density. For all of the simulations, the kinetic/internal energy ratio remains well below the 10% limit. None of the density choices were able to accurately capture the behavior of the

material, but changing the density does not appear to impact the final result within the specified limits. Densities of 993E4 kg/m³ and 994E2 kg/m³ will be used for future simulations in testing sensitivity of other parameters.

6.4 Initial Fiber Volume Fraction Sensitivity Analysis

Due to discrepancies in the density of the kenaf fiber, the calculation of the actual fiber volume fraction was uncertain. As previously stated, sources have listed the density of kenaf to be between 0.25 and 0.44 g/cm³. Kenaf fiber is grown in nature, and the density may vary from plant to plant depending on the growing conditions. For this reason, sensitivity analysis has been completed for different initial fiber volume fractions. The given range of fiber density gives initial fiber volume fractions between 0.4 and 0.6. The results from these simulations have shown that, qualitatively, not much difference is seen in the numerical solution. Table 6.2 summarizes the results.

Table 6.4 Initial Fiber Volume Fraction Sensitivity Analysis Results

Initial Fiber Volume Fraction	Number of Wrinkles	Maximum Internal Energy (Joules)	Maximum Kinetic Energy (Joules)
0.4	14	9 E9	1.75
0.5	14	12 E9	2.2
0.6	16	16 E9	3.2

By increasing the initial fiber volume fraction, the composite is being stiffened. The more fiber in the composite, the stronger the material and the more energy it will have. This expected result is illustrated by the increase of

both the internal energy and the kinetic energy of the blank. A comparison of the formed composite with each of the three initial fiber volume fractions is shown in Figure 6.5. The model with using 0.6 shows two more wrinkles than the 0.4 and 0.5 volume fractions. Note the wrinkles are larger, each taking up more of the circumference of the outer edge, in the 0.4 and 0.5 models. This behavior is closer to the experimental behavior than the smaller, closely packed wrinkles shown in the model with a 0.6 initial fiber volume fraction. Choosing the density of kenaf fiber to be at the median of the given range yields an initial fiber volume fraction of approximately 0.5. This value has been chosen to be used for all future simulations.

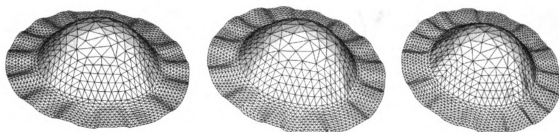


Figure 6.7 Comparison of numerical results with initial fiber volume fractions of 0.4 (left), 0.5 (center), and 0.6 (right)

6.5 Shear Modulus Sensitivity Analysis

The next parameter that was analyzed is the Shear Modulus. As discussed in Chapter 4, no experimental method or literature was available to determine the value of the Shear Modulus of the kenaf fiber. The best estimate available was to use the isotropic assumption. As shown in the previous figures, the material is not isotropic, which discredits the assumption of using the isotropic model to calculate the Shear Modulus. Unfortunately, no other data

was available. A sensitivity analysis has been completed on this parameter to determine the effect of changing the Shear Modulus has on the results.

Table 6.5 Shear Modulus Sensitivity Analysis Results

Shear Modulus (Pa)	Number of Wrinkles	Maximum Internal Energy (Joules)	Maximum Kinetic Energy (Joules)
1.43 E6	14	1.1 E10	2
1.43 E7	14	1.1 E10	2
1.43 E9	14	1.2 E10	2.2

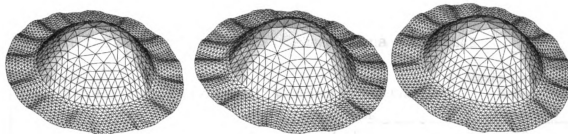


Figure 6.8 Comparison on numerical results with Shear Modulus of 1.43E6 Pa (left), 1.43E7 Pa (center), and 1.43E9 Pa (right)

From the data shown in Table 6.3 and Figure 6.6, there is no significant difference in the model when changing the Shear Modulus between 10^3 orders of magnitude. It has been concluded that the behavior of the material is not heavily dependent on the Shear Modulus; therefore, the proposed isotropic model will be sufficient for the data in this model. The Shear Modulus value will remain at 1.43E9 Pa for future simulations.

6.6 Transverse Shear Stiffness Sensitivity Analysis

The final parameter which has been tested for sensitivity is the Transverse Shear Stiffness. This parameter was calculated directly from the Shear Modulus that was examined in the last section. Due to the fact that no sensitivity to the Shear Modulus was determined, it is expected that the originally chosen value for the Transverse Shear Stiffness will be correct. In addition to the expected value of 1.23E6 Pa, values at magnitudes of 10^3 above and below have been examined.

Table 6.6 Transverse Shear Stiffness Sensitivity Analysis Results

Transverse Shear Stiffness (Pa)	Number of Wrinkles	Maximum Internal Energy (Joules)	Maximum Kinetic Energy (Joules)
1.23 E6	14	1.2 E10	2.2
1.00 E3	uncountable	4 E7	2.4
1.23 E9	14	1.6 E10	20

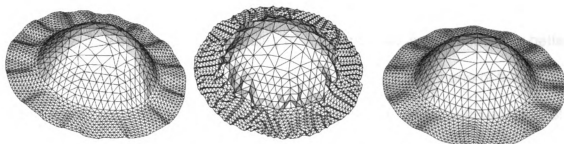


Figure 6.9 Comparison of numerical results with Transverse Shear Stiffness of 1.23E6 Pa (left), 1.00E3 Pa (center), and 1.23E9 Pa (right)

The results of this comparison show that the chosen transverse shear stiffness value of 1.23E6 Pa will be sufficient for analysis. Using the smaller (1.00E3 Pa) value obviously did not provide enough stiffness. Using a higher






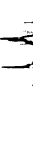

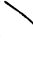






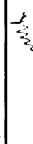
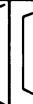
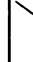



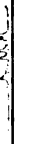
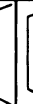
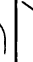

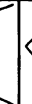
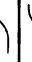

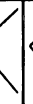
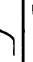


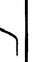
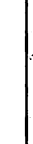














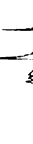





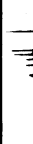


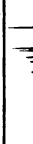
value provided the same qualitative results, but a much higher maximum kinetic energy. No change in the wrinkling behavior has been noted between the reasonable stiffness values.

6.7 Numerical Analysis Final Results

Sensitivity analysis has been performed on all of the variables that could have possibly been influencing the behavior of the model. None of the changes produced significant variance in the output except for the transverse shear stiffness, discussed earlier. Each of the simulations produced resultant parts with between 13 and 17 wrinkles. The desired result was to have only 6 wrinkles. Table 6.1 is a summary of the results for all the simulations.

As shown in Table 6.1, the kinetic energy behavior remained as desired for all of the simulations, leveling off to zero and staying fairly minimal. The internal energy behavior could be converted to a quasi-static situation by changing the punch amplitude from step amplitude to saw tooth amplitude. Additionally, it was found that increasing the total simulation time allows for better internal energy behavior with more leveling off. Unfortunately, none of the models tested gave the same results as experimentation. After exhausting all of the possible changes that could be made to the properties it must be concluded that the current model is unable to capture the behavior of the material. Suggestions for more appropriate models will be discussed in Chapter 8.

Table 6.7 Summary of Numerical Simulation Results

ODB	Density kg/m ³	Initial Fiber Volume Fraction	Shear Modulus (Pa)	Transverse Shear Stiffness (Pa)	Total Simulation Time (seconds)	Punch Amplitude	Number of Wrinkles	IE Max (J)	IE Trend	KE Max (J)	KE Trend
1	993 E4	0.4	1.43 E9	1.23 E6	0.3		17	9.00E+09		1.75	
2	993 E4	0.5	1.43 E9	1.23 E6	0.3		16	1.20E+10		2.4	
3	993 E4	0.6	1.43 E9	1.23 E6	0.3		15	1.70E+10		6	
4	993 E4	0.5	1.43 E6	1.23 E6	0.3		15	1.00E+10		1.75	
5	993 E4	0.5	1.43 E7	1.23 E6	0.3		13	1.00E+10		3	
6	993 E2	0.5	1.43 E6	1.23 E6	0.3		13	1.40E+08		0.7	
7	993 E2	0.5	1.43 E9	1000	0.3		uncountable	4.00E+07		2.4	
8	993 E2	0.5	1.43 E9	1.23 E6	0.3		13	1.20E+08		1.7	
9	993 E2	0.5	1.43 E9	1.23 E6	0.1		14	1.20E+08		2	
10	993 E4	0.5	1.43 E9	1000	1		uncountable	4.00E+07		2	
11	993 E6	0.5	1.43 E9	1.23 E6	1		15	1.20E+12		4.5	
12	993 E2	0.5	1.43 E9	1.23 E6	0.5		15	1.20E+08		2.2	
13	993 E2	0.5	1.43 E9	1.23 E6	1		14	1.20E+08		2.5	
14	993 E4	0.4	1.43 E9	1.23 E6	1		14	9.00E+09		1.75	
15	993 E4	0.5	1.43 E9	1.23 E6	1		14	1.20E+10		2.2	
16	993 E4	0.6	1.43 E9	1.23 E6	1		16	1.60E+10		3.2	
17	993 E4	0.5	1.43 E6	1.23 E6	1		14	1.10E+10		2	
18	993 E4	0.5	1.43 E7	1.23 E6	1		14	1.10E+10		2	
19	993 E4	0.5	1.43 E6	1000	1		uncountable	3.50E+09		2.5	

Chapter 7

NEW DIE DESIGN

Much experimental work has now been done by our research group on the four-inch hemispherical punch. In order to further prove the strengths of stamp thermo-hydroforming and the formability of the kenaf-polypropylene composites, a new die must be designed. This design will increase the versatility in making different shapes and sizes of part using the stamp thermo-hydroforming process.

7.1 Design Features

One of the acclaimed benefits of the stamp thermo-hydroforming process is the ability to form parts into complex shapes. The hemispherical punch shows the three dimensional formability of a part, but more complex shapes need to be formed. Additionally, in the current press, there is room to make parts larger than four inches. The goal in designing the new dies and punch is to make the design extremely flexible and able to accommodate the largest parts possible with interchangeable punches. An assembly view of the new design will be shown first in Figure 7.1, followed by a description of the features of each new design.

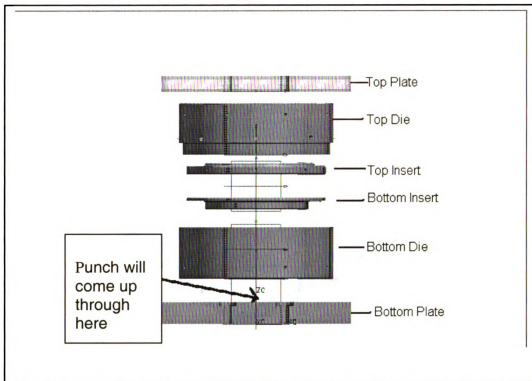


Figure 7.1 New die design, exploded view

The first parts that will be discussed will be the top and bottom plates. These are essentially the same as the original design, just scaled up to utilize all the space available and make the largest parts possible. The only additional feature that has been added to these plates is two additional slots on the sides for more secure fastening of the plates to the press. The hole in the bottom plate has also been increased from a 3" diameter to a 4" diameter to enable the punch base to be able to come up into the bottom plate and allow more draw depth when forming. The hole in the top plate has not been changed and remains at ¼" NPT to be used for instrumentation. Additionally, the drain hole in the bottom plate has been enlarged to account for the increase in fluid volume during

hydroforming. This will help with the larger die to enable the cavity to drain more quickly.

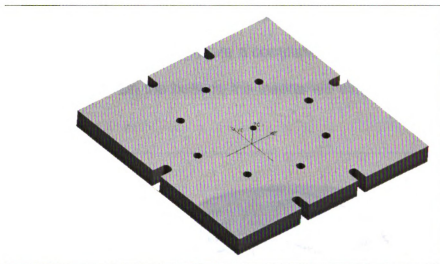


Figure 7.2 New design of top plate

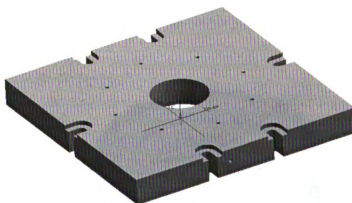


Figure 7.3 New design of bottom plate

The top and bottom dies were directly modeled after the revised design completed by Nader Abedrabbo that was used for the experimentation in this study. The same methods of fastening have been employed, along with the

same holes around the outer perimeters of the dies used for instrumentation. The largest difference with the new dies is the way they have been broken down and now will feature additional inserts. The inserts screw in from the outer sides on the top die in order to insure a completely flush surface for the formed part to move against. On the bottom, the inserts will simply screw in from the center of the die.

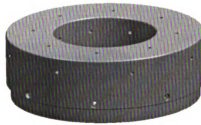


Figure 7.4 New design of top die



Figure 7.5 New design of bottom die

It is easily seen from Figure 7.5 that the inserts will fit into the dies, keeping the center hole the same radius, and add a uniform thickness on the

forming surface. The added thickness will make the height of the forming surfaces equal to the height of the lips that fit together. By using these inserts, it is much easier to change to different punch shapes and form more complex parts by also changing the shape of the insert. The first new design has just been a scaled up version of the original design; therefore, the first inserts designed have simply been circular.

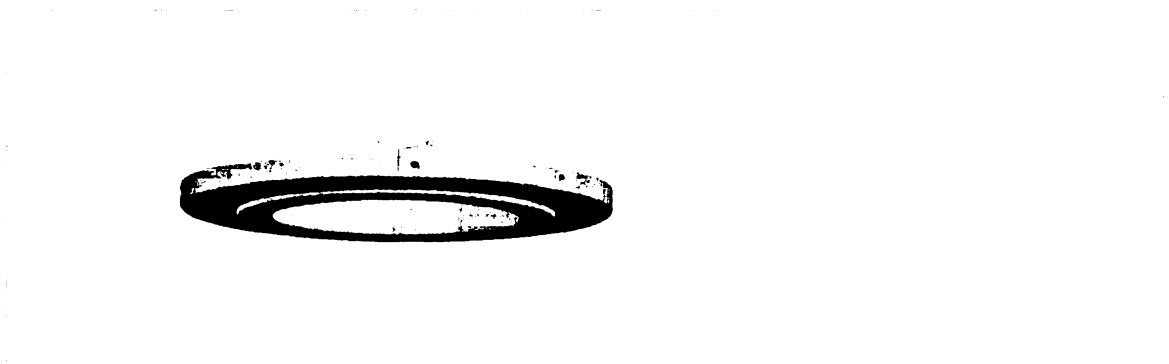


Figure 7.6 New design of insert

7.2 Punch Options

The desired first option for the punch at this time is a scaled down oil pan. The double curvature of the feature will give the opportunity to show the variety of forming abilities of the stamp thermo-hydroforming process. A sample oil pan was supplied to the research group by Dr. John Carsley of General Motors Corporation. Figure 7.7 shows the original oil pan design that is currently used in production in comparison with the simplified and miniaturized design that has been completed for use in later experiments.

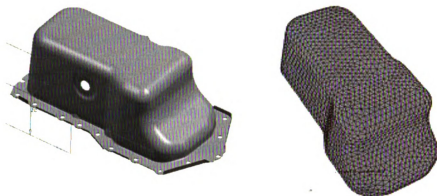


Figure 7.7 Original oil pan design and modified oil pan for formability tests

As shown in the figure the bottom lip has been removed from the original design as well as the holes in the sides. The goal of this research will be to show the possibility of forming such complex geometry as the double curvature shown using the stamp thermo-hydroforming process. By using a simplified model, the time and cost of simulation and actual formation will be decreased substantially.

With such a rectangular punch shape, the material may not perform well with a larger circular die opening. For this reason, the inserts featured in the design become important. Simulations will be run with both a circular die opening and also using the newly designed inserts that are in the same shape as the top profile of the oil pan punch. These inserts were designed by basically tracing the form of the punch from the top view and enlarging it to give a clearance of 1.1 times the thickness of the material to be formed. In this case, the material will be the kenaf-PP/MAPP composites with a thickness of 2mm; therefore, the clearance will be 2.2mm.

Chapter 8

CONCLUSIONS

The research done in this study has proven the ability to successfully fabricate kenaf-polypropylene natural fiber composites. The optimal fabrication method for the compression molding process has proven to be the layered “sifting” of a microfine polypropylene powder and chopped kenaf fibers. A fiber content of 30% by weight has been proven to provide adequate reinforcement to increase the strength of the polypropylene powder. The use of the coupling agent, 3% Epolene G3015 from Eastman Chemical Company, has enabled successful fiber-matrix adhesion.

Squeeze flow testing was used to determine two of the preferred fiber orientation for the composite. For a random chopped fiber kenaf composite, the preferred fiber orientations are at 40° and 170°. Material properties of the composite were then determined based on these two directions.

The kenaf-PP composites compression molded in this study proved to have superior tensile and flexural strength in the directions of the two preferred fiber orientations. When compared to other compression molded natural fiber composites, the kenaf composites manufactured in this study outperformed other kenaf, sisal, and coir composites in terms of Tensile Strength. The kenaf-PP-MAPP composites also outperformed all of those composites as well as hemp in the flexural test.

With the elastic modulus data from testing, it was also possible to compare the benefits of using this kenaf composite over other natural fibers as well as E-glass. The kenaf-PP-MAPP composites manufactured in this study have a higher Modulus/Cost and a higher Specific Modulus than sisal, coir, and even E-glass.

Preliminary experiments with the in-house stamp thermo-hydroforming equipment have proven successful. Preform circles with a 6.5" diameter were successfully thermoformed into hemispherical cups with a draw depth of 4 inches. It was found that the die must be at an elevated temperature as well as the preform in order to prevent cooling and tearing during forming. Further experimentation is necessary to determine the full scope of applications, which may utilize this new material.

In parallel with the preliminary experimentation, the design of a new, larger die set for testing was also completed. The new die set will utilize all of the available forming space within the existing Interlaken Press. With the new design, performs may be as large as 12" diameter circles, rather than the previous 7" maximum. Additionally more versatility in terms of punch shapes has been designed in to the new dies. Instead of being one solid piece with a circular opening, the dies have been broken into two pieces, one being the majority of the die, and the other being an exchangeable insert.

The benefit of having interchangeable inserts is the versatility of being able to change the punch without re-designing the entire die. The new die was designed with a circular opening, as in the original design. However, a new

punch design, modeled after a scaled oil pan, has required matching inserts to be designed. The oil pan shaped inserts enable better forming of the part, giving only 1.1*thickness of the material for clearance. Utilizing a new punch design will assist in demonstrating more forming options for the kenaf composites manufactured in this study.

Numerical simulation of the behavior of the kenaf-PP-MAPP composites was attempted using the finite element commercial code ABAQUS. The natural fiber composite material was modeled using a VUMAT originally created by Michael Zampaloni. The model was originally created to model the behavior of random orientation chopped fiber glass-mat composites. The version of this model that was used for simulation included numerical inputs of material characteristics for two chosen preferred fiber orientations and was based on a linear elasticity model.

Outrageous computation times for the full model led to a mass/density scaling analysis of the model. It has been shown that scaling the density does not have a large impact on the qualitative resultant formed part. Densities of magnitudes from E2 to E6 showed little change in the predicted number of wrinkles. For this reason, the density was scaled for all future numerical work. Sensitivity analysis has been performed on all of the variables that could have possibly been influencing the behavior of the model. None of the changes produced significant variance in output, except the transverse shear stiffness, discussed earlier. Each of the simulations produced resultant parts with between 13 and 17 wrinkles. The desired result was to have only 6 wrinkles. It has been

concluded that the current numerical model is not capable of accurately capturing the behavior of the kenaf-PP-MAPP composites.

Much more work may be done to further improve the composite properties as well as the numerical model. According to the findings in this research, compression molded kenaf natural fiber-polypropylene composites manufactured using the sifting method is a viable solution for substitution for current composites. These composites will be useful in order to make more environmentally friendly components in automobiles, airplanes, and possibly structural applications.

Chapter 9

FUTURE WORK

With this data as a starting point, much more work may be done with the kenaf-PP/MAPP composites. Both experiments with the present experimental set-up as well as with the new die design could be performed to get a better idea of how these composites behave. More numerical work and analysis is necessary to find an appropriate way to model the behavior of this material.

9.1 Future Manufacturing Experimentation

While the kenaf-polypropylene-Epolene G3015 composites manufactured for this research showed good properties, there is still much room for improvement. Most definitely the chopping, cleaning, and sifting process of the kenaf should be automated using a line cutter and screen. Automating these processes would save an enormous amount of time and, therefore, money. The automated chopping and screening would help to ensure and maintain a specified characteristic fiber length. Also, screening would assist in making sure that the fibers are in fact randomly placed in a repeatable fashion for more material property consistency. This could possibly add to the strength of the composites as well.

Another possible way to add to the strength of the composites would be to use an alkaline solution treatment on the fibers in addition to the maleated

polypropylene coupling agent. The compression molding process should be able to outperform composites made by previous processes such as resin transfer molding and extrusion followed by injection molding. Compression molding is a one step process and it does not place extreme shear forces on the fibers. If the optimal bond is formed between the fiber and the matrix, compression molding will be the optimal manufacturing method. It has already been shown in Chapter 2 that the use of a coupling agent and an alkaline treatment on the fibers increased strength in other natural fiber composites [27]. The next step to increasing properties of these composites is to incorporate the use of an additional alkaline fiber treatment. Once these composites are manufactured, they may be tested and compared to the composites utilizing only MAPP to determine the additional benefits of using the alkaline solution.

The final future kenaf composite manufacturing step will be to incorporate a biodegradable polymer. The goal of this work with kenaf natural fiber is to create more usable components that are environmentally friendly. Both the automotive and aerospace industries have become increasingly interested in using more biodegradable materials. There still exists a concern that the material will maintain the desired properties throughout its lifetime, yet be biodegradable when use is finished. This concern may be placated by the use of metallic sandwich structures with biocomposite filler/reinforcement. Further experimentation is necessary to determine the challenges and benefits of creating biocomposite sandwich structures.

9.1 Future Forming Experimentation

In addition to improving the composites themselves, more preliminary forming experimentation must be completed. At this point, only simple hemispherical forming with a wrinkling die has been completed. The composites have shown good formability when retained at the melt temperature of 190°C. Next, more experiments must be run to find the maximum draw depth, the behavior with a holding force exerted, as well as the formability when using the hydroforming capability of the current in-house stamp thermo-hydroforming machine.

The new die design will soon be installed to enable experimentation on forming much larger parts. The oilpan shaped punch will be used to illustrate the degree of formability of the kenaf-PP/MAPP composites. The large geometrical changes and radii of curvature will aid in proving the effectiveness and diversify the possible uses of this material. The next step will also be to use this new design to test the ability to form sandwich structure biocomposite parts into this complex geometry.

9.2 Future Numerical Work

One of the most important steps that must next be completed is to find a constitutive model that will be able to capture the behavior of this composite accurately. Michael Zampaloni has created updated version of the two preferred fiber orientation material VUMAT that now can incorporate three or four preferred fiber orientations. From the squeeze flow testing done in this work, two more

preferred fiber orientations may be chosen in order to improve the accuracy of the numerical model. Experimental tests must be completed once again with respect to the new preferred fiber orientations in order to populate the three and four preferred fiber orientation models.

With the updated models, sensitivity analysis must be completed once again to make sure all of the inputs are correct and that mass/density scaling does not affect the results immensely. If, by using the more specific three and four preferred fiber orientation models, the experimental wrinkling behavior is still not captured, then it must be concluded that the linear elasticity model is not adequate. Different types of material behavior models must be tested. It is possible that the kenaf composites exhibit a behavior closer to a viscoelastic material instead of a linearly elastic material behavior.

REFERENCES

- [1] Joshi S.V., Drzal L.T., Mohanty A.K., and Arora S., "Are natural fiber composites environmentally superior to glass fiber reinforced composites?", *Composites: Part A* 35 (2004) P. 371-376.
- [2] Mohanty A.K., Misra M., and Drzal L.T., "Sustainable Bio-Composites from Renewable Resources: Opportunities and Challenges in the Green Materials World", *Journal of Polymers and the Environment* Vol. 10, Nos1/2 (2002) p. 19-26.
- [3] Zampaloni M., "Investigation of Prior Research Activities and Current Practices for Processing Multi-Material Layered Structures Utilizing Biocomposites", Internal Michigan State University Report (2003).
- [4] Mohanty A.K., Drzal L.T., and Misra M., "Novel hybrid coupling agent as an adhesion promoter in natural fiber reinforced powder polypropylene composites", *Journal of Materials Science Letters* 21 (2002) p.1885-1888.
- [5] Mohanty A.K., Misra M., and Drzal L.T., "Green composites – value added agricultural products from biofibres and bioplastics", *Abstracts of Papers of the American Chemical Society* 225: U983-U984 207-IEC Part 1 (2003).
- [6] Baiardo M., Zini E., and Scandola M., "Flax fibre-polyester composites", *Composites: Part A* 35 (2004) p. 703-710.
- [7] Rouison D., Sain M., and Couturier M., "Resin transfer molding of natural fiber reinforced composites: cure simulation", *Composites Science and Technology* 64 (2004) p. 629-644.
- [8] Mehta G., Mohanty A.K., and Drzal L.T., "Biobased resin as a toughening agent for biocomposites", *Green Chemistry* 6-5 (2004) p. 254-258.
- [9] Parikh D.V., Calamari T.A., Sawhney A.P.S., Blanchard E.J., Screen F.J., Myatt J.C., Muller D.H., and Stryjewski D.D., "Thermformable automotive Composites Containing Kenaf and Other cellulosic Fibers", *Textile Research Journal* 72-8 (2002) p. 668-672.
- [10] Bledzki A.K. and Faruk O., "Wood Fibre Reinforced Polypropylene Composites: Effect of Fibre Geometry and Coupling Agent on Physico-Mechanical Properties", *Applied Composite Materials* 10 (2003) p. 365-379.
- [11] George J., Klompen E.T.J, and Peijs T., "Thermal degradation of green and upgraded flax fibres", *Advanced Composites Letters* 10-2 (2001) p. 81-88.

- [12] Villar J.C., Poveda P., and Tagle J.L., "Comparative study of kenaf varieties and growing conditions and their effect on kraft pulp quality", *Wood Science and Technology* 34-6 (2001) p. 543-552.
- [13] Zampaloni M.A., "Experimental and numerical study of stamp hydroforming for processing glass mat fiber reinforced thermoplastic sheets", Michigan State University (2000).
- [14] Zampaloni M.A., "A multi-preferred fiber orientation constitutive model for fiber mat reinforced thermoplastics with a random orientation applied to the stamp thermo-hydroforming process", Michigan State University (2003).
- [15] Zampaloni M., Pourboghrat F., and Yu W., "Stamp Thermo-Hydroforming: A New Method for Processing Fiber Reinforced Thermoplastic Composite Sheets", *Journal of Thermoplastic Composite Materials*
- [16] McKenzie, A.W. and Yuritta J.P., "Wood fibre reinforced polymers", *Appita* Vol. 32 No. 6 (1979) p. 460-465.
- [17] Michell, A., "Composites containing wood pulp fibres", *Appita* Vol.39 No. 3 (1986) p.223-229.
- [18] Mohanty A.K., Misra M., and Hinrichsen G., "Biofibres, biodegradable polymers and biocomposites: An overview", *Macromolecular Materials and Engineering* 276/277 (2000) p. 1-24.
- [19] Wambua P., Ivens J., and Verpoest I., "Natural fibres: can they replace glass fibre reinforced plastics?", *Composites Science and Technology* 63 (2003) p. 1259-1264.
- [20] Mishra S., Mohanty A.K., Drzal L.T., Misra M., Parija S., Nayak S.K., and Tripathy S.S., "Studies on mechanical performance of biofibre/glass reinforced polyester hybrid composites", *Composites Science and Technology* 63 (2003) p. 1377-1385
- [21] Mohanty A.K., Wibowo A., Misra M., and Drzal L.T., "Effect of process engineering on the performance of natural fiber reinforced cellulose acetate biocomposites", *Composites: Part A* 35 (2004) p. 363-370.
- [22] Nishino T., Hirao K., Kotera M., Nakamae K., and Inagaki H., "Kenaf reinforced biodegradable composite", *Composites Science and Technology* 63 (2003) p. 1281-1286.

[23] Lopez C., Information packet sent along with samples, Vision Paper: A Division of KP Products Inc., Albuquerque, NM, Phone: (505)294-0293, Fax: (505)294-7040, Email: INFO@VISIONPAPER.COM, Website: www.visionpaper.com

[24] Burgueno R., Quagliata M.J., Mohanty A.K, Mehta G., Drzal L.T., and Misra M., "Load-bearing natural fiber composite cellular beams and panels", Composites: Part A 35 (2004) p. 645-656.

[25] George J., Sreekala M.S., and Thomas S., "A Review on Interface Modification and Characterization of Natural Fiber Reinforced Plastic Composites", Polymer Engineering and Science Vol. 41, No. 9 (2001) p.1471-1485.

[26] Feng D., Caulfield D.F., and Sanadi A.R., "Effect of Compatibilizer on the Structure-Property Relationships of Kenaf-Fiber/Polypropylene Composites", Polymer Composites Vol. 22, No. 4 (2001) p. 506-517.

[27] Mohanty A.K., Drzal L.T., and Misra M., "Engineered natural fiber reinforced polypropylene composites: influence of surface modifications and novel powder impregnation processing", Journal of Adhesion Science Technology Vol. 16, No. 8 (2002) p. 999-1015.

[28] Keener T.J., Stuart R.K., and T.K Brown, "Maleated coupling agents for natural fibre composites", Composites: Part A 35 (2004) p. 357-367.

[29] Mase T., Drzal L. and Jurek B. , "Development of a Heat/Pressure Formable Wood Fiber Thermoplastic Composite From Recycled Paperboard",

[30] Bhattacharyya D., Bowis M. and Jayaraman K., "Thermoforming woodfibre-polypropylene composite sheets", Composites Science and Technology 63 (2003) p. 353-365.

[31] Yu W.R., Pourboghrat F., Chung K., Zampaloni M., and Kand T.J., "Non-orthogonal constitutive equation for woven fabric reinforced thermoplastic composites", Composites: Part A 33 (2002) p. 1095-1105.

[32] Yu, (2003)

[33] Dong L., Lekakou C., Bader M.G., "Processing of Composites: Simulations of the Draping of Fabrics with Updated Material Behaviour Law", Journal of Composite Material 35 (2001) p.138-163.

[34] Mohammed U., Lekakou, C., and Bader, M.G., "Experimental studies and analysis of the draping of woven fabrics", Composites: Part A 31 (2000) p.1409-1420.

[35] Mase G.T. and Mase G.E., Continuum Mechanics for Engineers, CRC Press LLC (1999) p. 227.

[36] ABAQUS Documentation 6.4

[37] Equistar Chemical Company website, Material Data Sheet for Microfine Polyolefin Powder-Polypropylene <http://www.equistarchemicals.com/TechLit/Performance%20Powders/FP809-00.pdf>

[38] Material database www.io.tudelft.nl/research/dfs/idemat/index.htm

[39] Sanadi A.R., Caulfield D.F., Jacobson R.E., and Rowel R.M., "Renewable Agricultural Fibers as Reinforcing Fillers in Plastics: Mechanical Properties of Kenaf Fiber-Polypropylene Composites", *Ind. Eng. Chem. Res.* 34 (1995) p. 1889-1896.

[40] Rowel R.M., Sanadi A., Jacobson R., and Caulfield D., "Properties of Kenaf/Polypropylene Composites", In: Kenaf Properties, Processing and Products; Mississippi State University, Ag and Bio Engineering, Chapter 32 (1999) p. 381-392.

[41] Davia D.J., Bagby M.O., Wolf B.A, Knowles P.F., and Goss J.R., "Cubing increases density of kenaf", *California Agriculture*, September (1978) p. 11-12.

[42] Adamson W.C. and Minton N.A., "Stem and Root Density in Kenaf and Roselle at Different Harvest Dates", *Crop Science* 21, November-December (1981) p. 849-851.

[43] Voulgaridis E., Passialis C., and Grigoriou A., "Anatomical Characteristics and Properties of Kenaf Stems (*Hibiscus Cannabinus*)", *IAWA Journal* 21 (4), (2000), p. 435-443.

[44] Webber III C.L., Blesdoe V.K., and Blesdoe R.E., "Kenaf Harvesting and Processing", Trends in New Crops and New Uses, J. Janick and A. Whipkey (eds.). ASHS Press, Alexandria, VA (2002).

[45] Seller Jr. T.S., Miller Jr. G.D., Fuller M.J., Broder J.G., and Loper II R.R., "Lignocellulosic-Based Composites Made of Core From Kenaf, An Annual Agricultural Crop", Conference of the International Union of Forest Research Organization, XX World Conference, Tampere, Finland (1995).

MICHIGAN STATE UNIVERSITY LIBRARIES



3 1293 02732 4809